A stochastic hydro-geomorphological model for shallow landsliding due rainstorm(Dissertation_全文)

AUTHOR(S):

Iida, Tomoyuki

学位申請論文

飯田　智之

A stochastic hydro-geomorphological model for shallow landsliding due to rainstorm

T. IIDA

Geo-Research Institute, Osaka Soil Test Lab., Itachibori Nishiku Osaka 550-0012, Japan

Abstract

A prediction model of shallow landsliding is proposed. It considers the stochastic aspects of intensity and duration of rainfall as well as the deterministic aspects containing slope stability, throughflow seepage and the development of regolith. It turns out that the probability of saturated throughflow, which is the direct trigger mechanism to shallow landsliding, can be expressed by a log-normal distribution. The short term probability of landsliding is defined as the excess probability that the depth of saturated throughflow surpasses the critical value. The average recurrence interval T_{av} of landsliding can be calculated as the expected value of recurrence interval of landslide.

This model was applied to a test field where a lot of shallow landsliding occurred at a heavy rainstorm in 1988. Then a DEM of 5-m grid interval was utilized to calculate T_{av} at every grid point. Consequently, it was found that the percentage of the landslide grid number to the total grid number for every T_{av} rank increases when T_{av} decreases. The spatial distribution of T_{av} reveals its significant dependence on the topography. Therefore, it is confirmed that T_{av} is a hydro-geomorphological index of the susceptibility to shallow landsliding.

keywords

stochastic process, landslide, slope stability, recurrence interval, DEM, hazard map

1. Introduction

Landsliding is a primary agent of landscape evolution in diverse regions. Especially in humid forested areas, such as Japan, shallow (at most 1 or 2 m deep) landsliding triggered by rainstorm seems to be the dominant denudational process on hillslopes. For example, Moriya (1972) and Shimokawa (1984) report numerous shallow landslide scars of various ages across the landscape. Shallow landsliding is important not only as a geomorphological process, but also as a cause of natural hazards. Therefore, the research on shallow landsliding has been carried out from the viewpoint of disaster prevention, rather than from a geomorphological one. According to these results, slope angle, slope shape (e.g., concave or convex) and the soil (regolith) depth are especially important as the controlling factors of shallow landsliding. In the 1970s, the hillslope hydrology approach was developed, and the saturated throughflow (shallow subsurface flow), which triggers shallow landsliding, was investigated (e.g., as compiled by Kirkby,1978). Hatano (1979) proposed a topographic index F ($=\tan\beta / (SCA)^{1/3}$) of susceptibility to shallow landsliding, where β is the slope angle, SCA is the specific catchment area. Okimura and his colleagues (e.g., Okimura and Ichikawa,1985; Okimura and Nakagawa,1988), and Montgomery and Dietrich (1994) developed successfully a DEM simulation model that coupled infinite slope stability analysis with seepage analysis.

On the other hand, valuable data about characteristics of "immunity" (a concept proposed by Koide (1955) in order to explain the tendency that the landsliding doesn't occur for a particular period after the former one) and periodicity of shallow landsliding, were collected in some regions since the 1980s, utilizing various methods of dendrochronology (Shimokawa, 1984; Shimokawa et al., 1989), tephrochronology (Yanai,1989; Yanai and Usui,1989a; Yanai and Usui,1989b; Yoshinaga and Saijo,1989; Yoshinaga et al., 1989; Shimizu et al., 1995), carbon 14 dating (Dietrich et al., 1986;

Reneau and Dietrich, 1987; Yoshinaga and Saijo, 1989; Yoshinaga et al., 1989) and aerial photos (Aniya,1985). Japanese data are compiled as shown in **Fig.1**. It is suggested that return period of shallow landsliding is influenced by both geology and slope angle. These data, although insufficient in number, stimulated the debate about the effect of geology and topography on the susceptibility to shallow landsliding. As for the effect of topography, Yanai (1989) found that both slope angle and slope shape (hollow or nose) are important factors for the average recurrence interval of shallow landsliding.

In order to estimate long term susceptibilities to shallow landsliding, a modelling of soil depth development and rainstorm occurrence is necessary, since both of them are controlling factors in the recurrence interval of shallow landsliding. In order to simulate the soil distribution and to estimate the root cohesion effect on the slope stability, Dietrich et al. (1995) developed Okimura's model utilizing a soil development model. Utilizing frequency distribution of rainstorm intensity and duration, a pioneering stochastic model was proposed by Dunne (1991) to simulate the past recurrence of shallow landsliding at a model hollow.

From the geomorphological view point, shallow landsliding can be regarded as one of stochastic processes, and the periodicity is the key property for prediction. In this paper, a stochastic process-based model (Iida,1999) is proposed, which has been improved on a previous one (Iida,1993). This model utilizes the slope stability analysis, seepage (saturated throughflow) analysis, soil development model and the statistics of rainstorm. Then, the methods of calculating the average recurrence interval T_{av} of shallow landsliding is proposed. Adopting this model to a test field utilizing a DEM, allows topographic effects on shallow landsliding to be compared.

This research is originated from Okunishi (1991,1994), in which the hydro-geomorphological methods for the research of geomorphology were proposed, and from

Dunne (1991), in which the stochastics of rainstorm was emphasaised on the hydro-geomorphological research of landslide.

2. Outline of test field and investigation methods

2.1 Outline of test field

The test field site is to the east of Hamada city in Shimane Prefecture. **Figure 2** shows the topography of the site (about 500m×800m area). The site is composed of gentle low-relief slopes surrounded by steep slopes. The bed rock is andesite. The wide distribution of relic red soil on gentle slopes, indicates that these gentle slopes have remained stable for a long time. The mean annual precipitation is about 1700 mm and the mean annual temperature is about 15℃. The area had been originally covered by cedar forests prior to clear cutting in the1970s. This area was hit by a heavy rainstorm on July 15th 1988, then a lot of shallow landslidings (at most 1 or 2 m deep) occurred, mainly on the steep slopes as shown in Fig. 2.

2.2 Investigation methods

In order to apply the stochastic process-based model proposed in this paper to the test field, observation of landslide scars, topographic analysis on DEM, soil depth measurement and some soil tests were carried out (Iida and Tanaka, 1997).

The DEM of 5-m grid interval is based on originally 1:1,000 topographic map with contour interval of 1-m prepared for the test field site after the 1988 disaster (**Fig.2**). **Figure 3** is a remaked map from the DEM. The grid point which falls into landslide scars (perhaps including some of the runoff scars) in 1988 are shown by solid triangle. Topographic features, such as slope angle β, laplasian $\nabla^2 h$, specific catchment area SCA are estimated at every grid point. Soil depth investigation was carried out with a

portable cone penetrometer. Open circles show the penetration test sites. N_{10} value is defined as the impact number of 5 kg weight, 50 cm free fall, needed to drive a cone every 10 cm. Physical properties and mechanical strength of the soil layer were estimated with conventional in-situ or laboratory methods. Hydraulic parameters which are usually difficult for us to measure were assumed by trial and error as shown in the section 3.2. The parameters of soil depth development model were assumed by referring data of other field sites as shown in the section 3.3.

3. Preparatory analysis model

3.1 Slope stability analysis model

Okimura and Tanaka (1980) made many investigations which showed that the depth of landsliding layer in the granitic areas, which had been experienced frequent shallow landsliding, can be determined by a simplified penetration test. They called this layer "the potential landsliding layer". They investigated the physical and mechanical properties of the potential landsliding layer and the boundary layer. Based on these results, Okimura and his colleagues developed successfully the simulation model of shallow landsliding using the two layer model of soil (regolith) and weathered bedrock (**Fig.4**). The two layer model is supported by many researchers of shallow landsliding, especially on the granitic slopes (e.g., Iida and Okunishi, 1983). The shallow subsurface flow, which occurs on the weathered bedrock, is supposed to be the direct trigger for shallow landsliding.

The bed rock of the test field site is not granite but andesite. Nonetheless, according to the observation of landslide scars in 1988 and the results of the penetration tests (Iida and Tanaka,1997), it is found ① that topographic features are the main factors of soil depth distribution, ② that the fundamental structures of ground is similar to those on the granitic area, that is, on the gentle low-relief slopes

the N_{10} value increases gradually with depth, on the other hand, on the steep slope N_{10} value is small (<5) up to a certain depth and increases suddenly at this depth, and ③ that the soil layer (defined as N_{10}<5) had been removed by shallow landsliding and the weathered bedrock (defined as N_{10} >5) was exposed. Therefore, the two layer model is applicable to the test field site, as well. The potential landsliding layer of the test field site can be defined as the soil layer with N_{10} < 5.

According to the stability analysis for the two layer model, the depth of saturated throughflow critical to shallow landsliding H_{cr} is written as

$$H_{cr} = \frac{c - \gamma_t \cos^2\beta(\tan\beta - \tan\phi)D}{\cos^2\beta\{(\gamma_{sat} - \gamma_t)(\tan\beta - \tan\phi) + \gamma_w \tan\phi\}} \quad (1)$$

where c is the cohesion, ϕ the internal friction angle, γ_t the unit weight of unsaturated soil, γ_{sat} the unit weight of saturated soil, γ_w the unit weight of water, β the slope angle and D the soil depth. Both H and D are measured to vertical direction (**Fig.4**).

On the basis of a sensitivity analysis, Okimura (1987) emphasizes that soil depth D is more important for occurrence of shallow landsliding than other factors, such as c or ϕ.

When the soil depth is equal to H_{cr}, the critical soil depth D_{im} is given as follows.

$$D_{im} = c \,/\, \cos^2\beta\{\gamma_{sat}(\tan\beta - \tan\phi) + \gamma_w \tan\phi\} \quad (2)$$

Assuming the soil cohesion $c > 0$, the geomorphological significance of soil depth D is given as follows (Iida,1993).

When the soil depth D is less than D_{im} (i.e. $H_{cr} > D$), the depth H of saturated

throughflow cannot reach the critical one H_{cr}, even at heaviest rainstorm. No shallow landsliding occurs, since the water table of saturated throughflow can not rise beyond the ground surface because of large permeability of the surface layer (A_0 layer). Because the period of $D < D_{im}$ corresponds to an "immunity" period (Shimokawa, 1984) of shallow landsliding, D_{im} may be named "immunity soil depth". When the soil depth D is greater than D_{im}, H can be larger than H_{cr} at a rainstorm, leading to shallow landsliding.

When the soil depth D is larger than D_{im} (i.e. $H_{cr} < D$), there are two cases as for relationship between D and H_{cr} (see eq. (1)).

In the case of relatively steep slope ($\phi < \beta$), H_{cr} decreases linearly with the increase of soil depth D, and H_{cr} eventually becomes zero. This means that shallow landsliding can occur on the slope without saturated throughflow if a critical ("upper limit") soil depth D_{ul} (corresponding to $H_{cr}=0$, and given as follows) is attained.

$$D_{ul} = c \,/\, \gamma_t \cos^2\beta (\tan\beta - \tan\phi) \qquad (3)$$

However, D_{ul} is never reached because soil depth increases slowly with time and periodic rainstorms will produce at least some saturated subsurface flow and consequently destabilization at thicknesses less than D_{ul}. According to this model, shallow landsliding occurs when the soil depth D ranges between D_{im} and D_{ul}.

In the case of relatively gentle slope, H_{cr} increases linearly ($\phi > \beta$) or remain constant ($\phi = \beta$) with increase of D, then no upper limit soil depth D_{ul} exists.

The sampling point of soil for soil tests is shown in **Fig.3**. The measured values of soil parameters of the potential landsliding layer were obtained as c =0.46 tf/m^2, ϕ =28.8 degs., γ_t =1.52 t/m^3 and γ_{sat} =1.69 t/m^3, respectively. These measured values

are very close to the values that Okimura and Ichikawa (1985) assumed at their test field, that is, c =0.5 tf/m^2, ϕ=31 degs. (tan ϕ=0.6), γ_t =1.7 t/m^3 and γ_{sat} =1.9 t/m^3, though the bed rock is not andesite but weathered granite. Additionally, soil parameters, such as c and ϕ, are not so important as soil depth or slope angle for slope stability (Okimura, 1987). Therefore, the rounded values of measured values, c =0.5 tf/m^2, ϕ=30 degs., γ_t =1.5 t/m^3 and γ_{sat} =1.7 t/m^3 as summarized in **Table 1** are assumed as the representative values in the test field site. These values are proved appropriate in section 3.2.

Using the assumed values, relationships of the critical depth H_{cr} of saturated throughflow and soil depth D are shown in **Fig. 5** for three sample slope angles, 40 degs. ($> \phi$=30 degs.), 30 degs. ($= \phi$), and 25 degs. ($< \phi$). The relationships of the immunity soil depth D_{im} and upper limit soil depth D_{ul} with slope angle β are shown in **Fig.6**. Open circles show the measured soil depth ($N_{10} < 5$).

3.2 Seepage analysis model

Judging from the fact that the hollow (i.e., zero order valley) is susceptible to shallow landsliding (e.g., Tsukamoto et al.,1982), the shallow subsurface flow or the saturated throughflow (Anderson and Burt,1978) seems to be the dominant factor for the occurrence of shallow landsliding.

In order to estimate the topographic effects on the saturated throughflow, a simplified method of seepage analysis is proposed on the assumption that the saturated throughflow flows parallel to bedrock, and that the recharge rate of the saturated throughflow is equal to the rainfall intensity (In other words, water loss, e.g., leakage through bedrock or retention of water to unsaturated zone, is negligible) (Iida,1984).

According to this method, the depth of saturated throughflow $H(t)$ is written as

$$H(t) = \int_0^{T_{max}} (da/d\tau) R(t-\tau) d\tau / (k \sin\beta \cos\beta) \quad (4)$$

where '$a(\tau)$' is the area in which the travel time of the saturated throughflow (the horizontal component of interstitial velocity = $k \sin\beta \cos\beta / n_e$) is up to τ, and $da/d\tau$ is "topographic" unit hydrograph, $R(t)$ the rainfall intensity at time t, T_{max} the maximum travel time of saturated throughflow, k the saturated permeability coefficient and n_e the "effective" porosity. The "effective" porosity represents the fraction of pore space that contributes to the quick response of the throughflow. It seems equivalent to specific yield as defined in groundwater hydrology.

Assuming that $R(t)$ is constant ($=I_0$) from $t=0$ to $t=t_1$, for the sake of simplicity, $H(t)$ is transformed as follows.

$$H(t) = I_0 a(t) / (k \sin\beta \cos\beta) \qquad (0<t<t_1) \quad (5)$$

$$H(t) = I_0 \{ a(t) - a(t-t_1) \} / (k \sin\beta \cos\beta) \qquad (t_1 \leqq t) \quad (5)'$$

The maximum depth H_{max} of saturated throughflow, doesn't occur necessaily at $t=t_1$ for hollow because of delay of water in arrival. Introducing $S_{max}(t_1)$ defined as the maximum value of $\{a(t) - a(t-t_1)\}$, H_{max} is given as

$$H_{max}(t_1) = I_0 S_{max}(t_1) / (k \sin\beta \cos\beta) \quad (6)$$

When water loss of saturated throughflow is not negligible, a modified topographic

unit hydrograph $da_{md}/d\tau$, which is assumed as follows for the sake of simplicity, can be substituted for $da/d\tau$ in eq.(4).

$$da_{md}/d\tau = da/d\tau \exp(-\alpha\tau) \tag{7}$$

where a_{md} is the modified covered area with the travel time, which is given by integrating eq.(7), and α the decay coefficient. In this case, $S_{max}(t_1)$ is re-defined as the maximum value of $\{a_{md}(t) - a_{md}(t-t_1)\}$.

Hydraulic parameters in the test field were estimated using actual data of shallow landsliding in 1988 as follows. The critical depth H_{cr} and the maximum depth h_{max} of saturated throughflow at 1988 disaster were calculated for grid points of two groups. The landslide grid group consists of all grid points within the 1988 landslide scars, while the non-landslide grid group consists of the grid points those are adjacent to the penetration test points shown in **Fig.3** by the open circles.

The values of H_{cr} (eq.(1)) demand data of soil depth. It is, however, difficult to estimate the original soil depth after landsliding. Therefore, it was assumed that original soil depth of the landslide grid group had been equal to the average of D_{im} and D_{ul} as shown by broken line in **Fig.6**. When the soil depth D of the non-landslide grid group is less than D_{im}, theoretically, no landslide occurs, and H_{cr} is considered infinite.

On the other hand, the values of h_{max} were calculated for all grids of two groups with eq.(4) substituting $da_{md}/d\tau$ for $da/d\tau$ and using the actual hyetograph on July 15th 1988 (**Fig.7**). The cumulative rainfall was about 350 mm in 6 hours. The return period of the rainfall ranges between 200 to 400 years according to duration (**Fig.14**). The topographic unit hydrograph $da_{md}/d\tau$ was estimated for each grid by using flow lines (see **Fig.3**).

The hydraulic parameters k, n_e and α were estimated by trial and error as follows. Theoretically speaking, the area where h_{max} is larger than H_{cr} corresponds to the unstable area, and another area where h_{max} is less than H_{cr} corresponds to the stable area. Many calculations were tried for various combination of k, n_e and α. Consequently, when hydraulic parameters are assumed as k = 0.1 cm/sec, n_e =20 (%) and α =0.4 (1/hour), the best hitting is achieved. The modified topographic unit hydrograph $da_{md}/d\tau$ are shown in **Fig.8** for three sample sites X,Y and Z in **Fig.3**.

The hitting result for each grid is shown in **Fig.9**. The hitting rate of non-landslide grid group is as large as 96 %. On the other hand, the hitting rate of the landslide grid group is 65 %. This value is not very high. The comparison of numbers of theoretical landslide grid points (Unstable area) and non-landslide grid points (Stable area) on actual landslide scars are shown in **Fig.10**. Landslide scar numbers (1 - 29) correspond to the numbers in **Fig.3**. All landslide scars excluding three scars (3,4 and 8) contain at least one dangerous grid point ($h_{max}>H_{cr}$). Some of non-landslide grid points may correspond to the runoff scars.

Consequently, the assumption that the soil of the test field site is hommogeneous as for mechanical, physical and hydrological properties, is proved appropriate, and these assumed values of parameters seem approximately correct in the test field site. These parameters are summarized in **Table 1**.

3.3 Soil depth development model

According to section **3.1**, soil (regolith) depth D is the very important factor for the occurrence of shallow landsliding. Additionally, from the view point of the long term prediction of landsliding, it is necessary to consider the time change of soil depth. Shimokawa (1984) investigated the reformation process of topsoil after landsliding on a granitic area with dendroclonology. He found that there were two reformation

processes of soil depth, i.e., the initial deposition process and weathering process and that weathering was more important than the initial deposition. Then he showed the development velocity of topsoil on landslide scars (open circles in **Fig.11**). His results suggest that the soil depth development is approximately expressed simply by a logarithmic function of time in a weathering dominant case containing initial deposition process as follows, although influenced by many kinds of physical, chemical and biological processes:

$$L(n)\ (=D\cos\beta) \quad = \quad A_w \ \ln\ (B_w n + 1) + L_0 \tag{8}$$

where $L(n)$ is the soil thickness (measured to normal direction to the slope.) n years after denudation by shallow landsliding, and A_w, B_w and L_0 are the constant parameters. L_0 corresponds to the initial deposition. By fitting eq.(8) to Shimokawa's data(1984), parameters were determined as shown in **Fig. 11** (Iida,1993). Trustrum and DeRose(1988) have proposed a similar logarithmic equation of soil development.

On the other hand, the following soil development model has been proposed by Ahnert (1966), and it states that weathering rate V_w is generally thought to decrease exponentially with the increase of soil thickness L.

$$V_w \quad = \mathrm{d}L/\mathrm{d}n = V_0 \exp(-\lambda L) \tag{9}$$

Equation (8) is a solution of eq. (9) where V_0 is $A_w B_w \exp(L_0/A_w)$ and λ is $1/A_w$.

Recently, the significance of slow mass movement on soil development in forested humid areas has been pointed out (e.g., Reneau et al., 1989; Dietrich et al., 1995; Sonoda and Okunishi, 1994; Yamada, 1997). Introducing V_c, which corresponds to the additional effect by slow mass movement, eq.(9) is revised as follows.

$$dL/dn = V_0 \exp(-\lambda L) + V_c \quad (9)'$$

V_c can be written as follows for soil creep (Culling, 1963; Hirano, 1968).

$$V_c = K \nabla^2 h \cos \beta \quad (10)$$

where K is the diffusion coefficient of soil creep and $\nabla^2 h$ the laplasian of elevation h. The values of $\nabla^2 h$ was calculated to estimate the values of V_c for every grids of DEM. If V_c is not zero and constant, the solution of eq. (9)' is given as follows.

$$n = \frac{1}{V_c \lambda} \left\{ (L - L_0) + \ln \frac{\{V_c + V_0 \exp(-\lambda L)\}}{\{V_c + V_0 \exp(-\lambda L_0)\}} \right\} \quad (11)$$

In the case that V_c is negative and the absolute value of V_c is less than V_0, substituting $dL/dn=0$ for eq. (9)', soil thickness for steady state L_{st} is given as

$$L_{st} = -\ln(-V_c/V_0) / \lambda \quad (12).$$

In order to estimate the soil depth development, we need weathering parameters A_w, B_w and L_0, and the diffusion coefficient of soil creep, K. However, in the test field, few data related to soil development was obtained. Therefore, values of A_w and L_0 in the test field were assumed to be 1.0m and 0.15m, respectively. These values are identical to those estimated from Shimokawa's data, which correspond to the case of V_c=0. According to observation on 1988 landslide scars, the average depth of initial deposition seems to attain the value similar to Shimokawa's result (0.15m).

The value of B_w was estimated as follows, using assumed values of diffusion coefficient K for soil creep and steady state soil thickness L_{st}. Dietrich et al.(1995) found out that the average value of K was 0.005m^2/yr for their test field sites. On the other hand, Nogami (1980) found out that the average value of K was 0.0059 m^2/yr in his test field. This approximate coincidence for K value is very interesting and important. It may be because both of their fields are located in humid forested areas, and slope length is similar to each other. Because climate, topography, vegetation of this test field is similar to their test fields, the value of K=0.005m^2/yr is eventually adopted.

Dietrich et. al. (1995) pointed out that the soil depth on a nose (ridge type slope) remains in a steady state based on the balance of the weathering rate of bedrock and denudation rate of the soil by the process of soil creep. This relation is written by eq. (12). According to the relationship between soil thickness L and $\nabla^2 h$ of slope in the test field, L_{st} is assumed to be 0.5 (m) at $\nabla^2 h = -0.1$ (1/m) (**Fig. 12**, Iida and Tanaka,1997).

Consequently, by substituting A_w=1.0m, L_0=0.15m, K=0.005m^2/yr, L_{st}=0.5m, $\nabla^2 h = -0.1$(1/m), $\cos\beta \fallingdotseq 1.0$, into eq.(10) and eq.(12) ($V_0 = A_w B_w \exp(L_0/A_w)$, $\lambda = 1/A_w$), the value of B_w was estimated as 0.0007 (1/yr). Using these parameters, the soil development curves for different values of V_c are shown in **Fig.13**.

4. Stochastic model of shallow landsliding

4.1 Statistics of rainstorm and saturated throughflow

The occurrence of rainstorms that trigger shallow landsliding is a random phenomenon; therefore, such type of processes should be treated stochastically (Dunne, 1991). A stochastic rainfall intensity-duration curve (Talbot type) is used, since most effective rainfall duration for saturated throughflow is different for each slope.

$$I(t_1,N) = a(N) / \{t_1 + b(N)\} \qquad (13)$$

where $I(t_1,N)$ is the average rainfall intensity (mm/h) of a storm with return period N (year) and rainfall duration t_1 (hour), $a(N)$ and $b(N)$ the parameters for N years probability.

After Ishiguro (1961), the parameters, $a(N)$ and $b(N)$ can be approximated by the following empirical equations.

$$b(N)=(24- I_{1N}/I_{24N}) / (I_{1N}/I_{24N}-1), \qquad a(N)=\{ b(N) + 24 \} I_{24N}$$

where I_{1N} is the annual maximum hourly rainfall and I_{24N} the annual maximum daily rainfall of N-years probability, respectively.

Using 100 years data from Hamada Meteorological Observatory, parameters $a(N)$ and $b(N)$ were calculated for appropriate values of N (=10,20,..,100,200,..,1000,2000,..). Consequently, it turned out that the values of $a(N)$ and $b(N)$ can be approximately written as power functions of N. Therefore, stochastic rainfall - duration curves in the test field can be expressed as follows.

$$I(t_1,N) = 124.6N^{0.24} / (t_1+2.22N^{0.077}) \qquad (13)'$$

The curves in **Fig.14** shows these functions for several probability years.

The probability of the occurrence of saturated throughflow is estimated as follows through seepage analysis in section **3.1** using hydrological parameters shown in **Table 1**. Substituting $I(t_1,N)$ for I_0 in eq. (6), $H_{max}(t_1)$ is transformed to

$$H_{max}(t_1,N) = S_{max}(t_1)\, I(t_1,N) \ / \ (k\sin\beta\cos\beta) \qquad (6)'$$

Consequently, N-years probability depth $H_N(N)$ is given as the maximum value of $H_{max}(t_1,N)$ for the rainfall duration t_1. $S_{max}(t_1)$, $H_{max}(t_1,N)$ and $H_N(N)$ at sample sites X,Y and Z (**Fig. 3**) are shown in **Fig. 15**. It is interesting and important that the rainfall duration t_1 corresponding to $H_N(N)$ are almost constant, irrespective of N. This is the case for most grid points in the test field. Introducing t_0 for the representative rainfall duration t_1 which corresponds to $H_N(N)$, $H_N(N)$ is transformed as follows.

$$H_N(N) = S_{max}(t_0) I(t_0,N) / (k \sin\beta \cos\beta) \tag{14}$$

This means that $H_N(N)$ is proportional to the rainstorm intensity $I(t_0,N)$ for a certain duration t_0, because $S_{max}(t_0)$ and $(k \sin\beta \cos\beta)$ in eq. (14) are independent of N.

The probability distribution of annual maximum rainfall intensity $I(t_1,N)$ for any duration t_1, can be expressed by a log-normal distribution similar to the daily (t_1=24) or the hourly (t_1=1) rainfall distribution. Therefore, it is apparent from eq.(14) ($t_1=t_0$) that the probability of saturated throughflow is able to be expressed by a log-normal distribution, too. These relationships are written as follows.

$$F(\xi) = \frac{1}{\sqrt{\pi}} \int_{-\infty}^{\xi/\sqrt{2}} \exp(-\xi^2) d\xi = \{ 1 + \mathrm{erf}(\xi / \sqrt{2}) \} / 2 \tag{15}$$

$$\xi = A'(t_0) + B'(t_0) \log (I(t_0,N)) \qquad \text{(rainfall intensity)} \tag{15'}$$

$$\xi = A + B \log (H_N) \qquad \text{(saturated throughflow depth)} \tag{15"}$$

where F is the non excess probability, $A'(t_0)$ and $B'(t_0)$ the parameters for rainfall intensity of duration t_0, A and B the parameters for saturated throughflow depth.

Consequently, the probability distribution of throughflow at any point can be characterized with only two hydro-geomorphological parameters of A and B in eq. (15)".

By substituting eq.(14) for eq.(15)" and comparing eqs. (15)' and (15)", the parameters for saturated throughflow are given by those for rainfall intensity as follows.

$$A = A'(t_0) - B'(t_0) \log \{ S_{max}(t_0) / (k \sin \beta \cos \beta) \}$$

$$B = B'(t_0)$$

The probability distribution of saturated throughflow depth are shown in **Fig.16** for three sample sites X,Y and Z in **Fig.3**. Although the specific catchment area SCA of Y site (190m) is smaller than that of Z site (295m), saturated throughflow depth of Y site is greater than that of Z site at any probability level. This is because N-years probability depth $H_N(N)$ is proportional to $S_{max}(t_0)$ defined as the maximum value of $\{a_{md}(t) - a_{md}(t - t_1)\}$ (see eq.(14)), and $S_{max}(t_0)$ isn't necessarily proportional to the specific catchment area SCA (see **Fig.15**) .

4.2 Probability of shallow landsliding

The steep slopes covered with soil mantle and vegetation, have alternately undergone either a removal of soil by shallow landsliding or an accumulation of soil by weathering or slow mass movement (such as soil creep) as shown by **Fig. 17**.

According to particle analysis, the soil (N_{10}<5) on the gentle slope which is unconditionally stable, is very mature (i.e. the main components are silt or clay), on the other hand, the soil on the steep slope is immature (i.e. the main components are

gravel and sand). This fact shows that shallow landsliding are frequent on the steep slopes in this area.

According to Iida (1993), the short term probability of landsliding Q, which is defined as the probability that shallow landsliding occurs within a year, can be expressed by eq. (16) as the excess probability that the depth of saturated throughflow surpasses H_{cr}.

$$Q = 1 - F(\xi(H_{cr})) \tag{16}$$

Q is an index of susceptibility of shallow landsliding from the point of view of short term prediction. The value of $1/Q$ is the return period of the rainstorm which causes landsliding. H_{cr} is a function of soil depth D, and D ($= L/\cos\beta$) is a function of time n (year). Therefore, Q is a function of n. The temporal change in the susceptibility to shallow landsliding can be expressed by the temporal change in Q value. While D is smaller than D_{im}, that is, in the immunity period, Q value is zero, therefore, no shallow landsliding occurs. When D is greater than D_{im}, Q value increase with time because H_{cr} decreases with increase in D in case of relatively steep slope ($\phi < \beta$) with the soil cohesion $c > 0$ (eq.(1)).

The long term probability of landsliding P, defined as the probability that landsliding occurs in a year between n and $(n-1)$ years after the last landsliding, can be expressed as follows.

$$P(n) = \{1-Q(1)\}\cdots\{1-Q(n-1)\}Q(n) \tag{17}$$

Average recurrence interval (T_{av}), average denudation rate (V_{av}) and average scar

depth (D_{av}) of shallow landsliding can be defined as follows, as the expected values, respectively.

$$T_{av} = \Sigma P(n)\, n \tag{18}$$

$$V_{av} = \Sigma P(n)\, \{D(n)/n\} - V_c/\cos\beta \tag{19}$$

$$D_{av} = \Sigma P(n)\, D(n) \tag{20}$$

where $D(n)$ is the soil depth n years after the last landsliding. In eq.(19), volumetric change ratio from rock to soil by weathering has been assumed to be 1.0.

The distribution map of T_{av} is regarded as a map of the relative susceptibility to shallow landsliding, from the point of view of the long term prediction based on hydro-geomorphology.

5. Model application and discussion

5. 1 Probability of saturated throughflow

The probability distribution of saturated throughflow was estimated for all grid points of slopes whose angles are greater than 20 degrees. Namely, the hydro-geomorphological values of A and B in eq. (15)" were calculated.

The correlation between A and B is shown in **Fig. 18**. It is clear that the variation of B is smaller than that of A. In other words, B doesn't depend on the topography so much as A. The spatial distribution of A value is shown in **Fig. 19**. The correlation between A and specific catchment area (SCA) is shown in **Fig. 20**. The correlation between A and laplacian $\nabla^2 h$ is shown in **Fig. 21**. Generally speaking, the smaller A value is, the larger the saturated throughflow depth is, for any probability level.

Therefore, A value is relatively small on hollow where SCA is large and $\nabla^2 h$ is positive. On the contrary, it is relatively large on nose where SCA is small and $\nabla^2 h$ is negative.

The inverse correlation is clear between A and SCA only for the range of less than 40 (m). This means that the area which contributes to the increase in the saturated throughflow depth is limited to just upslope area, where the equivalent distance (= SCA) is less than 40 m, for the intense rainfall with short duration. Of course, the contributing area depends on hydraulic parameters k, α and n_e, however, the total area of SCA doesn't necessarily contribute to increase in saturated throughflow depth in the case of relatively large SCA and for the rainstorm with short duration.

5.2 Average recurrence interval of shallow landsliding

The average recurrence interval T_{av} of landsliding was calculated with the method shown in section **4.2**, utilizing the mechanical and hydrological parameters in **Table 1**, the soil depth development model in section **3.3**, and the hydro-geomorphological parameters of A and B estimated in section **5.1**.

The time change of the long term probability P and the average recurrence interval T_{av} of landsliding are shown in **Fig.22** for three sample sites X,Y and Z (**Fig.3**). If the depth of saturated throughflow $H_N(N)$ is large enough at any probability year N, landslides occur as soon as the soil depth reaches D_{im} (immunity soil depth), since Q and P immediately take high values. This is the case for sites Y and Z. Therefore, T_{av} is strongly controlled by soil development. However, if $H_N(N)$ is small at any probability year N, landslides seldom occur just after the soil depth reaches D_{im}. This is the case for sites X. Then, T_{av} is controlled by the probability of the occurrence of a saturated throughflow, as well as the soil development.

The distribution of T_{av}, which is classified into several ranks, is shown in **Fig.23**. Cases of T_{av} larger than 10,000 years is, for the sake of convenience, classified to the

same rank as non-landsliding. The values of T_{av} shown in **Fig.23** seem reasonable in Japan (see **Fig.1**). The values of T_{av} are small (less than 1000 years) for the steep slopes and the hollow type slopes which are known empirically to be most susceptible to shallow landsliding. Because the soil in the test field site has been assumed to be homogeneous as for the mechanical, hydrological parameters and the parameters of soil development, variation of the values of T_{av} shown in **Fig. 23** is attributable to those of topography. Therefore, the value of T_{av} is approximately expressed as follows by a regression to representative topographic factors,: slope angle β, laplasian $\nabla^2 h$ and hydro-geomorphological parameter A.

$$\log(T_{av}) = 4.28 - 0.047\beta - 2.68\nabla^2 h + 0.226A \qquad (r=0.97) \qquad (21)$$

Figure 24 represents the distribution of the average recurrence interval T_{av}. In about 30% grid points of this test field, shallow landslides can occur with T_{av} less than 10,000 years. The shadowed bar graph represents the frequency of the 1988 landslide grid points. There are some problems, : the data from only one particular disaster event had been applied, and the landslide grid points might contain runoff (secondary landsliding) scars. However, it has to be highlighted that the rate (percentage) of the number of 1988 landslide grid points to that of total grid numbers for every T_{av} rank is supposed to be a kind of susceptibility index to landsliding. This index is shown by dots in **Fig. 24.** Inverse correlation between this index and T_{av} is reasonable.

Figure 25 shows the histogram of the grid point number (%) of T_{av} for different slope angle ranks. The value of T_{av} is widely distributed when the slope angle is small. It is interesting that the percentage of stable rank grids (containing grid points of T_{av} >10,000 years) changes drastically at the slope angle of 35 degs.. In other words, this shows that susceptibility to shallow landsliding increases suddenly over 35 degs.. As

for susceptibility of shallow landsliding, Takeshita (1985) already pointed out the significance of this boundary angle based on his abundant field observation. Yanai(1989) also supported Takeshita's view based on the tephrochronological data. Although the bed rock of this test field is different from those of their test fields, this coincidence of the boundary slope angle of shallow landsliding is interesting.

The distribution of average denudation rate V_{av}, which is classified into several ranks, is shown in **Fig. 26**. It is clear that the values of V_{av}, as well as those of T_{av}, depend on the topography.

6. Conclusions

A long term prediction model of shallow landsliding, which considers not only the deterministic aspects but also the stochastic aspects of rainstorm, is proposed. According to the stability analysis, shallow landsliding occurs when the depth of saturated throughflow rises above the critical one, H_{cr}, on condition that the soil depth D is between two critical values, i.e., the immunity soil depth D_{im} ($H_{rc}=D$) and the upper limit soil depth D_{ul} ($H_{cr}=0$).

The probability of saturated throughflow can be estimated by the indirect method using a simplified seepage analysis (topographic unit-hydrograph method) and the stochastic rainfall intensity-duration curve. According to this model, the particular rainfall duration exists for each slope, which causes the highest water table of throughflow. The total area of specific catchment area (*SCA*) doesn't necessarily contribute to the highest stage of saturated throughflow table. Additionally, the probability of saturated throughflow can be approximated by a log-normal distribution function, analogously to that for rainfall intensity.

The short term probability of landsliding Q which is defined as the probability that shallow landslide occurs within a year, is equal to the probability that the

saturated throughflow depth surpasses H_{cr}. While D is smaller than D_{im},, Q value is zero, therefore, no shallow landsliding occurs. When D is greater than D_{im}, Q value increase with time because H_{cr} decreases with increase in D in case of relatively steep slope ($\phi < \beta$) with the soil cohesion $c > 0$.

The average recurrence interval T_{av} of shallow landsliding can be estimated as expected value of the recurring period n of landsliding by using the long term probability $P(n)$ (which is defined as $\{1-Q(1)\}\cdots\{1-Q(n-1)\}Q(n)$). Although, strictly speaking, this model should be applied only to the spontaneous landslide scars, T_{av} can be mapped in order to show the spatial distribution of shallow landsliding susceptibility. It was confirmed using actual data of landslide, that the smaller the value of T_{av} is, the larger the susceptibility to landsliding is. Additionally, T_{av} can be approximately expressed by a regression to representative topographic factors: slope angle β, laplasian $\nabla^2 h$ and hydro-geomorphological parameter A. The distribution map of T_{av} can be regarded as a hydro-geomorphological activity map of shallow landsliding.

The calculation of T_{av} needs data of ① the mechanical, physical and hydrological properties of soil layer, ② the soil development, ③ the stochastics of rainfall and ④ DEM (at most10m grid intervals). Generally speaking, although it is not necessarily easy to gain those data for every site at present, the process based model of shallow landsliding seems to have a future.

On the other hand, the value of $1/Q$ is the return period of the rainstorm which causes landsliding. Therefore, if data of soil depth are additionally available from all places, the distribution map of Q or $1/Q$, which is calculated using eq. (1) and eq. (16), is regarded as the more useful hazard map for the present (a short term prediction).

Basis of this paper

This thesis is based on the following papers;

Iida,T.,1984, A hydrological method of estimation of the topographic effect on the saturated throughflow. Trans. Japanese Geomorph. Union, 5, 1-12 (in Japanese with English abstract).

Iida,T.,1993, A probability model of the slope failure and the hillslope development. Trans. Japanese Geomorph. Union, 14, 17-31 (in Japanese with English abstract).

Iida,T.,1999, A stochastic hydro-geomorphological model for shallow landsliding due to rainstorm. Catena, 34 , 293-313 (in press).

The first paper proposed hydro-geomorphological methods in order to estimate topographic effects on the saturated throughflow. The second paper established the concepts of short term probability and long term probability of shallow landsliding. The last paper proposes a long term prediction model of shallow landsliding, which considers both the deterministic aspects containing slope stability, seepage of saturated throughflow and soil depth development, and the stochastic aspects of rainstorm.

Acknowledgements

The manuscript has greatly benefited from many comments by Professor Kazuo Okunishi of Disaster Prevention Research Institute, Kyoto University, and Professor William E. Dietrich of Department of Geology and Geophysics, University of California.

The author wishes to thank Dr. Kohei Tanaka of National Research Institute for Earth Science and Disaster Prevention, Science and Technology Agency for valuable help of field works, Professor Yukinori Matsukura of the University of Tsukuba for valuable help of laboratory works and for useful comments, and Dr. Carlos Barrientos S., Ministry of Energy and Mines, Caracas, Venezuela for his critique of the manuscript.

The author would also like to express his sincere gratitude to President Koichi Akai, Director Yoshinori Iwasaki and other members of the Osaka Soil Test Laboratory for their kind support.

References

Ahnert,F,1966, Zur Rolle der elektronischen rechenmachine Modells in der Geomorphologie. Geographische Zeitschrift,5,118-133.

Anderson,M.G., and Burt,T.P.,1978, The role of topography in controlling throughflow generation. Earth Surface Processes,3,331-344.

Aniya M.,1985, Contemporary erosion rate by landsliding in Amahata river basin, Japan. Z.Geomorph.N.F.29.301-314.

Culling,W.E.H,1963, Soil creep and the development of hillside slopes. J.Geor.,71,127- 161.

Dietrich,W.E., Wilson,C.J., and Reneau,S.L.,1986, Hollows, colluvium and landslides in soil-mantled landscapes. In Abrahams, A.D. ed., Hillslope Processes, Allen & Unwin,London,361-388.

Dietrich W.E., Reiss R., Hsu M. and Montgomery D.R.,1995, A process-based model for colluvial soil depth and shallow landsliding using digital elevation data. Hydrological Processes,9,383-400.

Dunne,T.,1991, Stochastic aspects of the relations between climate, hydrology and landform evolution. Trans. Japanese Geomorph. Union,12 ,1-24.

Hatano S., 1979, Classification of erosional topography in post glacial age and a method of prediction of the site of landslide. Proceedings of Japan Society of Erosion Control Engineering,16-17. (in Japanese).

Hirano,M.,1968, A mathematical model of slope development: an approach to the analytical theory of erosional topography. J. Geo-Sciences Osaka City Univ.,11, 13-52.

Iida,T.,1984, A hydrological method of estimation of the topographic effect on the saturated throughflow. Trans. Japanese Geomorph. Union, 5,1-12 (in Japanese with English abstract).

Iida,T.,1993, A probability model of the slope failure and the hillslope development. Trans. Japanese Geomorph. Union, 14,17-31 (in Japanese with English abstract).

Iida,T.,1996, A probability model of the slope failure based on soil depth distribution. Trans. Japanese Geomorph. Union, 17,69-88 (in Japanese with English abstract).

Iida,T.,1999, A stochastic hydro-geomorphological model for shallow landsliding due to rainstorm. Catena, 34 , 293-313 (in press).

Iida,T. and Tanaka K.,1997, The relationship between topography and soil depth measured with the portable penetration test apparatus. Trans. Japanese Geomorph.Union,18,61-78 (in Japanese with English abstract).

Ishiguro M.,1961, On the estimation of probable rainfall intensity formula by specific coefficient methods. Trans. Japan Society of Civil Engineers,74,19-26 (in Japanese with English abstract).

Kirkby,M.J. (ed.) ,1978, Hillslope Hydrology. John Wiley and Sons, 389p.

Koide H.,1955, Yamakuzure (landslide), Kokon-shoin, 205p.(in Japanese).

Montgomery D. R. and Dietrich W. E.,1994, A physically based model for the topographic control on shallow landsliding. Water Resources Research,30,1153-1171.

Moriya I.(1972) Classification of mountainous topography based on form of landslide as slope unit and slope development. Proceedings of the Association of Japanese Geographers, Volume Chiriyo 2,168-169. (in Japanese).

Nogami M.,1980, Numerical calculation and its explanation of "DIFFUSION" coefficient for slope evolution of terrace cliff during these hundred thousand years. Geographical Review of Japan,53,636-645. (in Japanese with English abstract).

Okimura T. and Tanaka S., 1980, Research on soil horizons of a weathered granite mountain slope and depth of the failed surface in a test field. Journal of the Erosion Control Engineering, Society of Japan, 116,7-16. (in Japanese).

Okimura T. and Ichikawa R.,1985, A prediction method for surface failures by movements of infiltrated water in a surface soil layer. Nat. Disaster Sci.,7,41-85.

Okimura T.,1987, Investigation and countermeasure of surface failures. "Chisitsu to tyosa",33-3,22-28. (in Japanese).

Okimura T. and Nakagawa M.,1988, A method for predicting surface mountain slope failure with a digital landform model. Journal of the Erosion Control Engineering Society of Japan, 41,48-56.

Okunishi,K.,1991, Hydrogeomorphological interactions - A review of approach and Strategy - . Trans. Japanese Geomorph. Union, 12, 99-116.

Okunishi,K.,1994, Concept and Methodology of Hydrogeomorphology. Trans. Japanese Geomorph. Union,15,5-18.

Reneau,S.L. and Dietrich,W.E.,1987, Size and location of colluvial landslides in a steep forested landscape. Internat. Assoc. Hydro.,Sci.Pub.,165,39-48.

Reneau,S.L.,Dietrich,W.E.,Rubin,M.,Donahue,D.J., and Jull,A.J.T.,1989, Analysis of hillslope erosion rates using dated colluvial deposits. J. Geol.,97,45-63.

Shimizu,O.,Nagayama T. and Saito M.,1995, Distribution and frequency of landslides for the last 8000 years in a small basin, Central Hokkaido. Trans. Japanese Geomorph. Union,16,115-136. (in Japanese with English abstract).

Shimokawa, E., 1984, A natural recovery process of vegetation on landslide scars and landslide periodicity in forested drainage basins. Proc. Symp. Effects of Forest land Use on Erosion and Slope Stability, Hawaii, 99-107.

Shimokawa,E., Jitousono,T. and Takano,S.,1989, Periodicity of shallow landslide on Shirasu(Ito pyroclastic flow deposits) steep slopes and prediction of potential landslide sites. Trans. Japanese Geomorph. Union,10,267-284. (in Japanese with English abstract).

Sonoda M. and Okunishi K.,1994, Downslope soil movement on a forested hillslope with granitic bedrock. Proceedings of the International Symposium on Forest Hydrology,479-486.

Takeshita K.,1985, Process of slope and soil formations on steep mountain slopes. Trans. Japanese Geomorph. Union,6, 317-332. (in Japanese with English abstract).

Trustrum,N.,A. and DeRose, R.C.,1988, Soil depth-age relationship of landslides on deforested hillslopes, TARANAKI,NEWZEALAND. Geomorphology,1,143-168.

Tsukamoto Y.,Ohta,T. and Noguchi, H.,1982, Hydrological and geomorphological studies of debris slides in Japan, Internal Assoc. Hydrol.Sci.Pub.,137,89-98.

Yamada S.,1997, Seasonal variation in soil creep on a forested hillslope near Sapporo, Hokkaido, northern Japan. Trans. Japanese Geomorph. Union,18,117-130.

Yanai S.,1989, Age determination of hillslope with tephrochronological method in Central Hokkaido, Japan. Trans. Japanese Geomorph. Union,10,285-301. (in Japanese with English abstract).

Yanai S. and Usui G.,1989a, Chronological analysis of the slope failure with the tephrochronological method - A history of the slope failure during the last 300 years on a disaster area -. Journal of the Erosion Control Engineering Society of Japan,42,5-13. (in Japanese with English abstract).

Yanai S. and Usui G.,1989b, Measurement of the slope failures frequency on sediments with tephrochronological analysis. Journal of the Erosion Control Engineering Society of Japan, 42,3-10. (in Japanese with English abstract).

Yoshinaga S. and Saijo K.,1989, Slope development during Holocene reconstructed process. Trans. Japanease Geomorph. Union,10,285-301. (in Japanese with English abstract).

Yoshinaga S., Saijo K. and Koiwa N.,1989, Denudation Process of mountain slope during Holocene based on the analysis of talus cone aggradation process. Trans. Japanese Geomorph. Union,10,179-193. (in Japanese with English abstract).

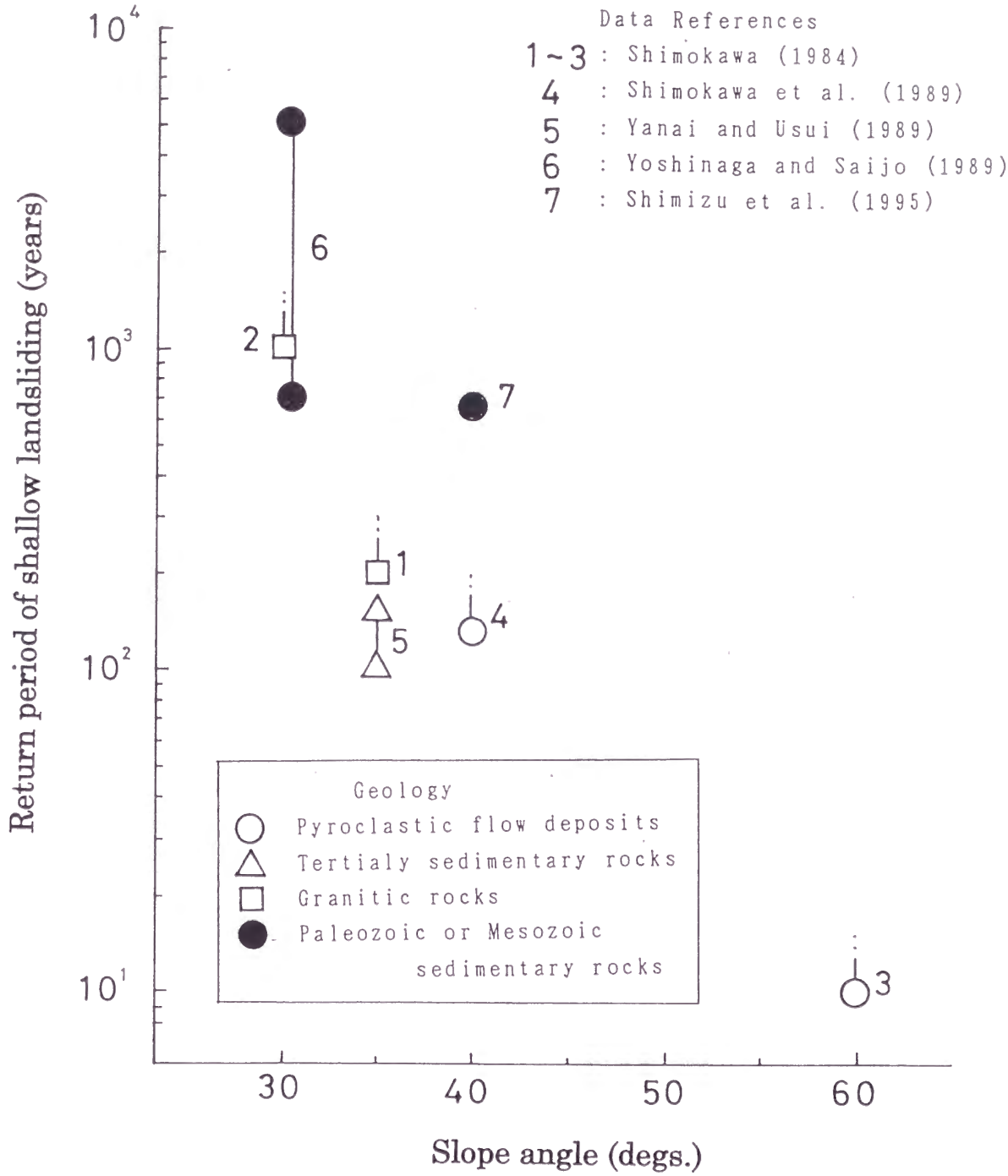

Fig. 1. The relationship between return period of landsliding with different geological conditions and slope angle. The return period was estimated with dendrochronological, tephrachronological or carbon 14 dating methods.

Fig. 2. A topographic map of the test field site.

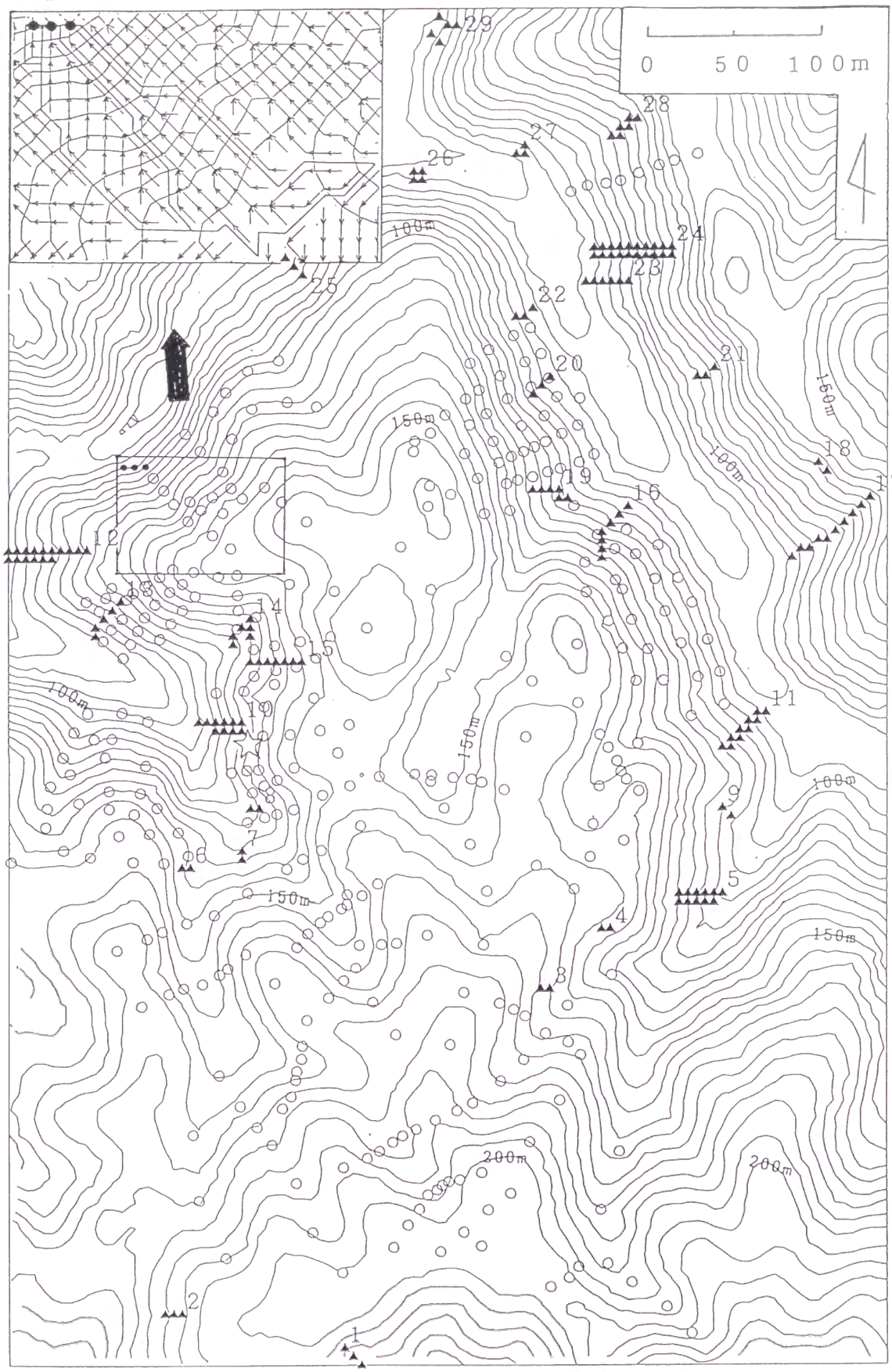

Fig. 3. A map of the test field which is remaked from DEM of 5-m grid interval and examples of flow lines (arrows). Open circles: penetration test sites, Triangles: landslide scars. Each triangle corresponds to a DEM grid point. Asterisk: sampling point of soil for soil tests.

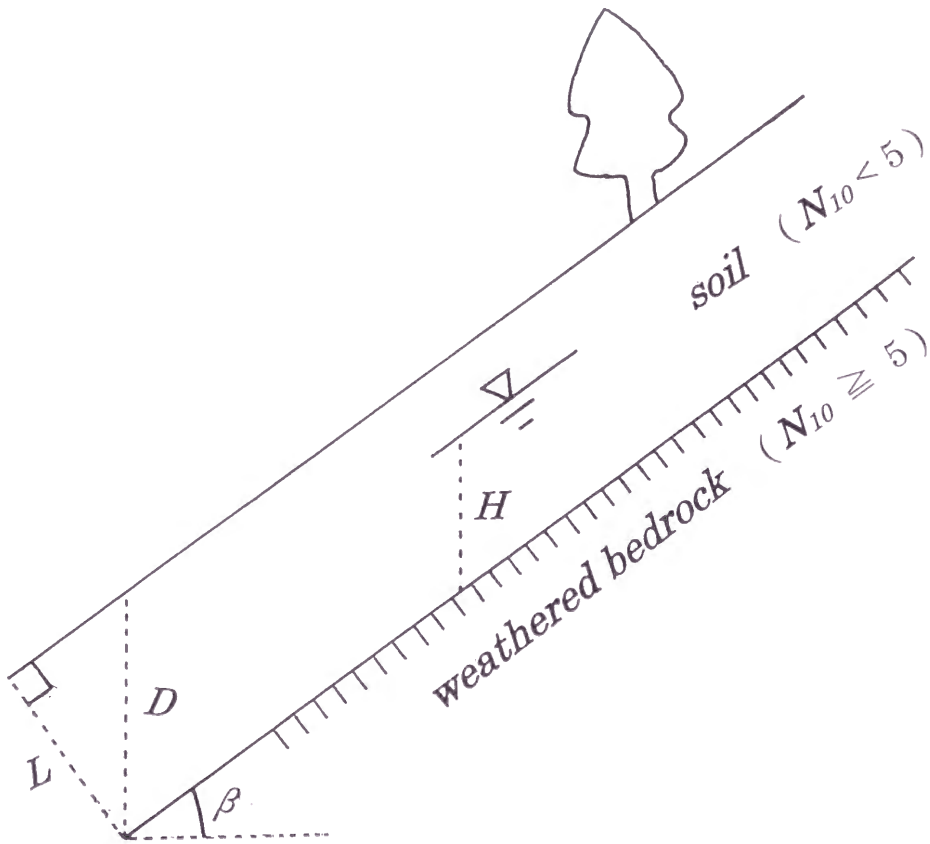

Fig. 4. Two layer model of the slope. The soil layer corresponds to "potential failure layer" defined by Okimura and Tanaka (1980).

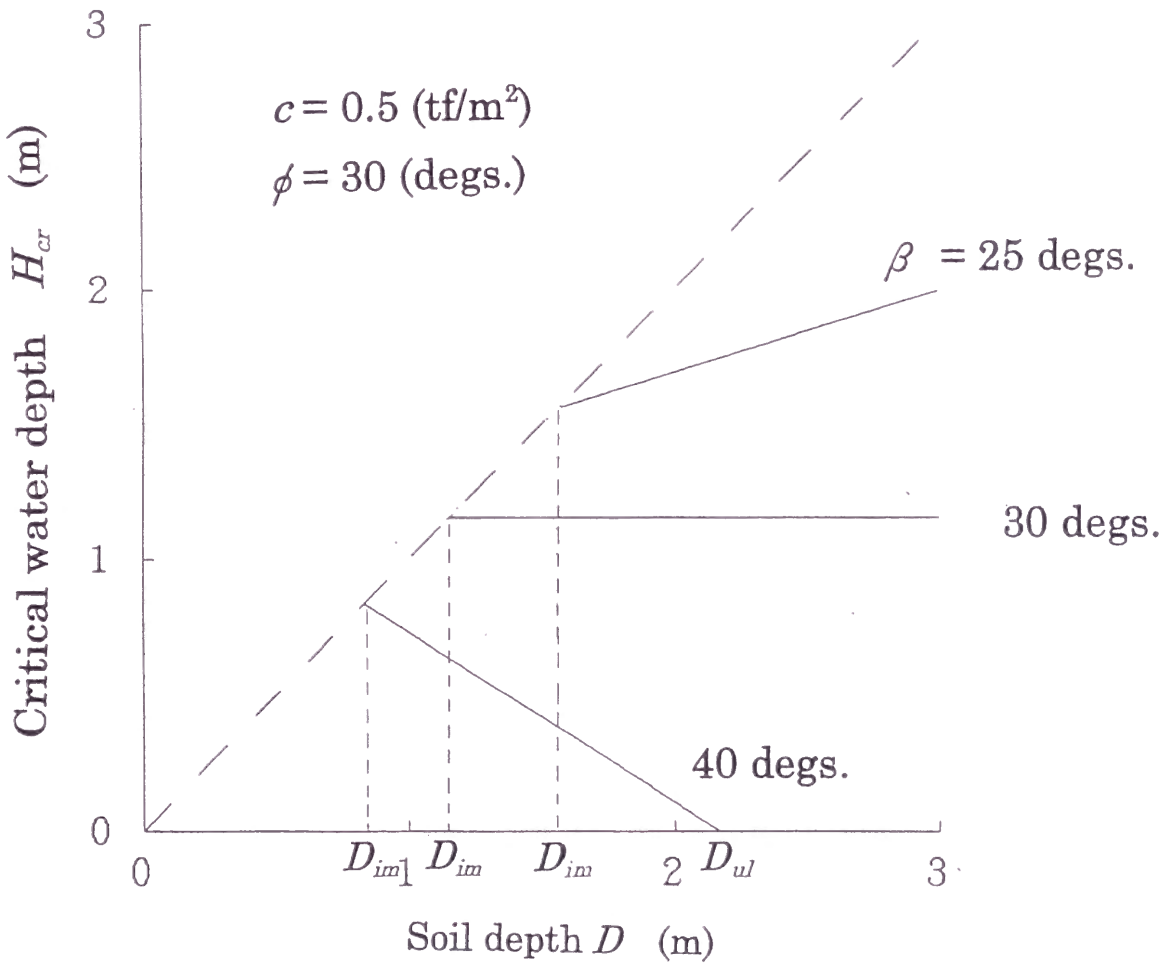

Fig. 5. The relationship between soil depth D and critical depth H_{cr} of saturated throughflow according to eq. (1) for slope angle, 25 degs., 30 degs. and 40 degs.

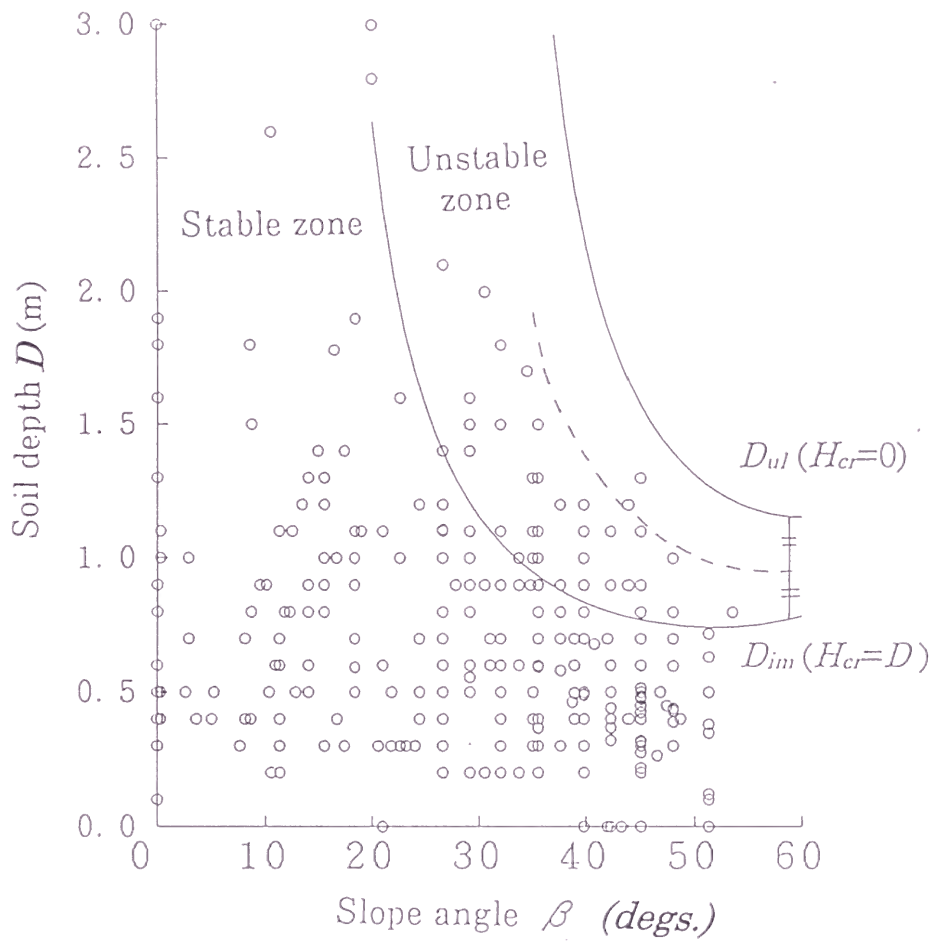

Fig. 6. The relationship between soil depth and slope angle. Open circles represent the field data.

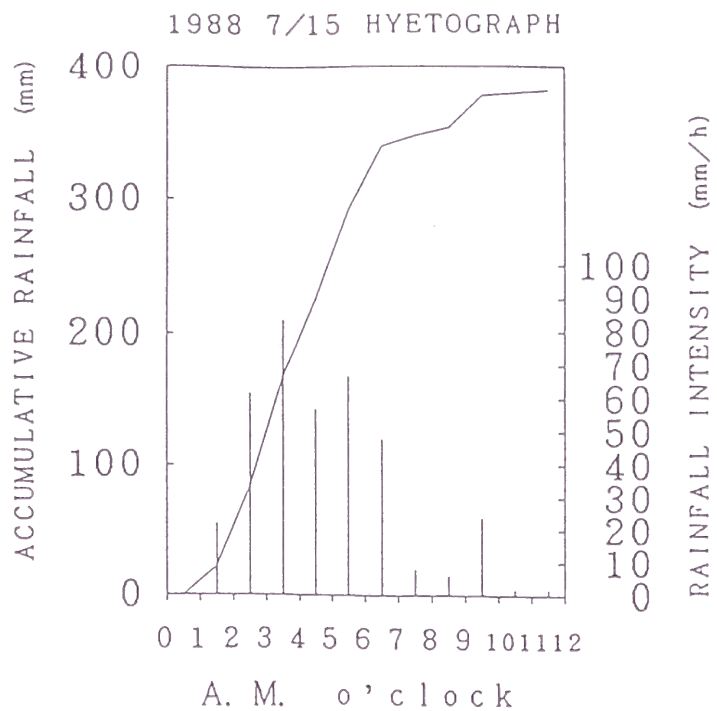

Fig. 7. The hyetograph at the 1988 rainstorm (after Hamada Meteorological Observatory).

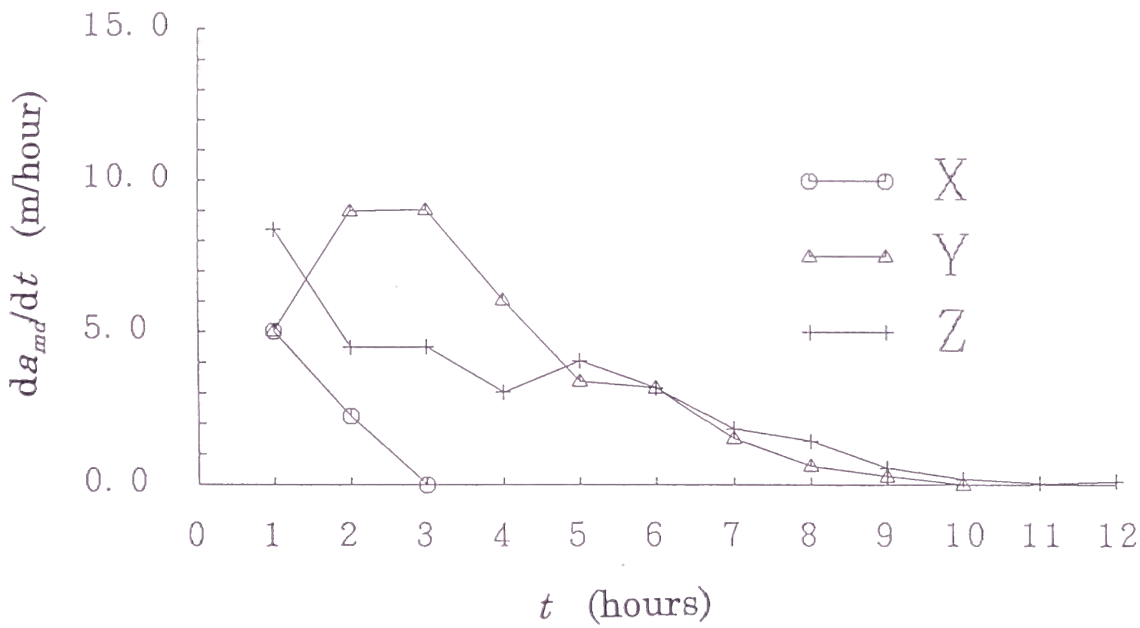

Fig. 8. Examples of modified topographical unit hydrograph. Three sites (X, Y and Z) are shown in Fig. 3. Hydraulic parameters are shown in Table 1.

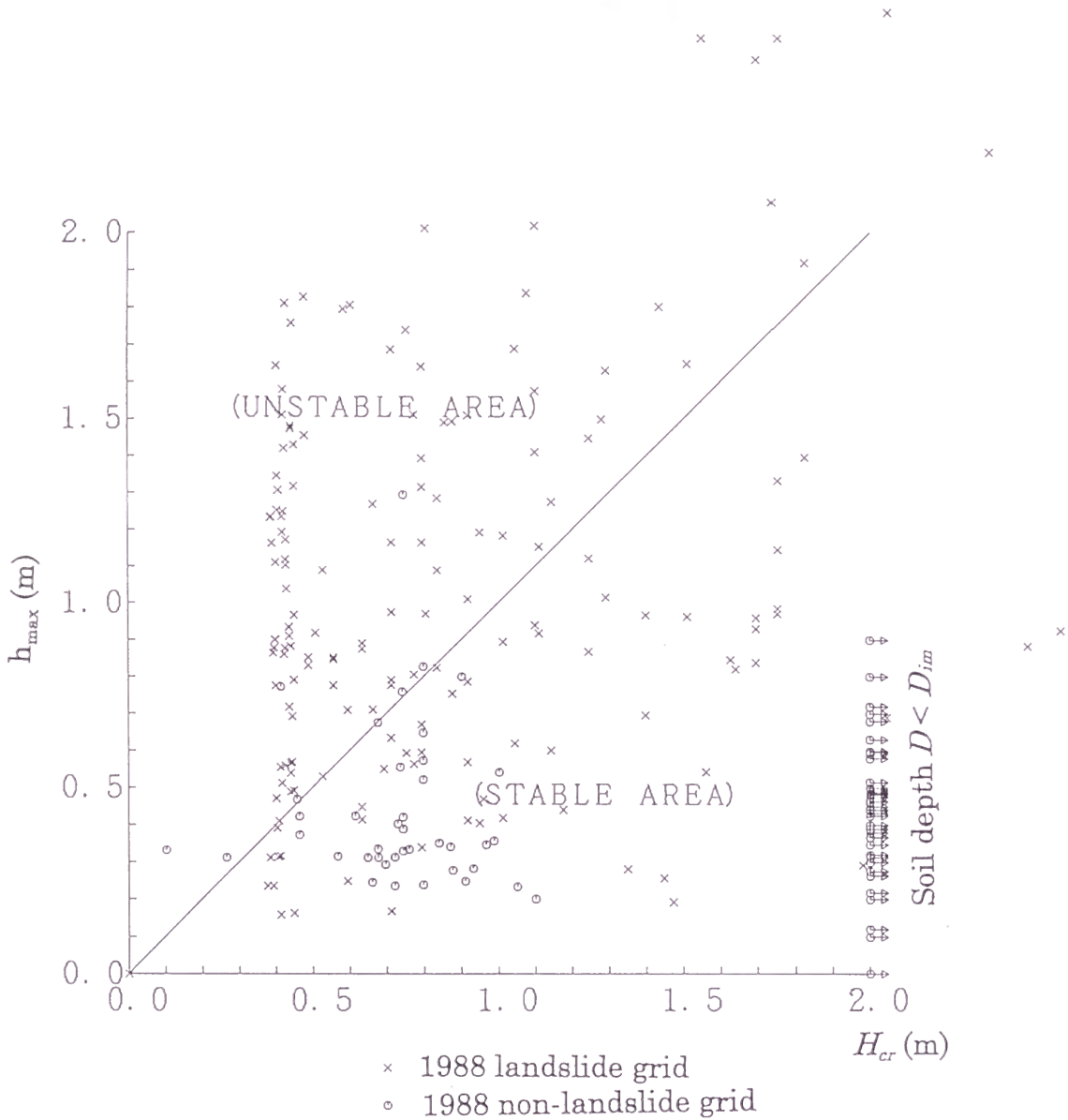

Fig. 9. The relationship between the critical throughflow depth H_{cr}, and the maximum throughflow depth h_{max} at the 1988 rainstorm on both of landslide grid points (X marks) and non landslide grid points (open circles). The lateral arrows show that H_{cr} is infinite because the soil depth D is less than D_{im}, the immunity soil depth.

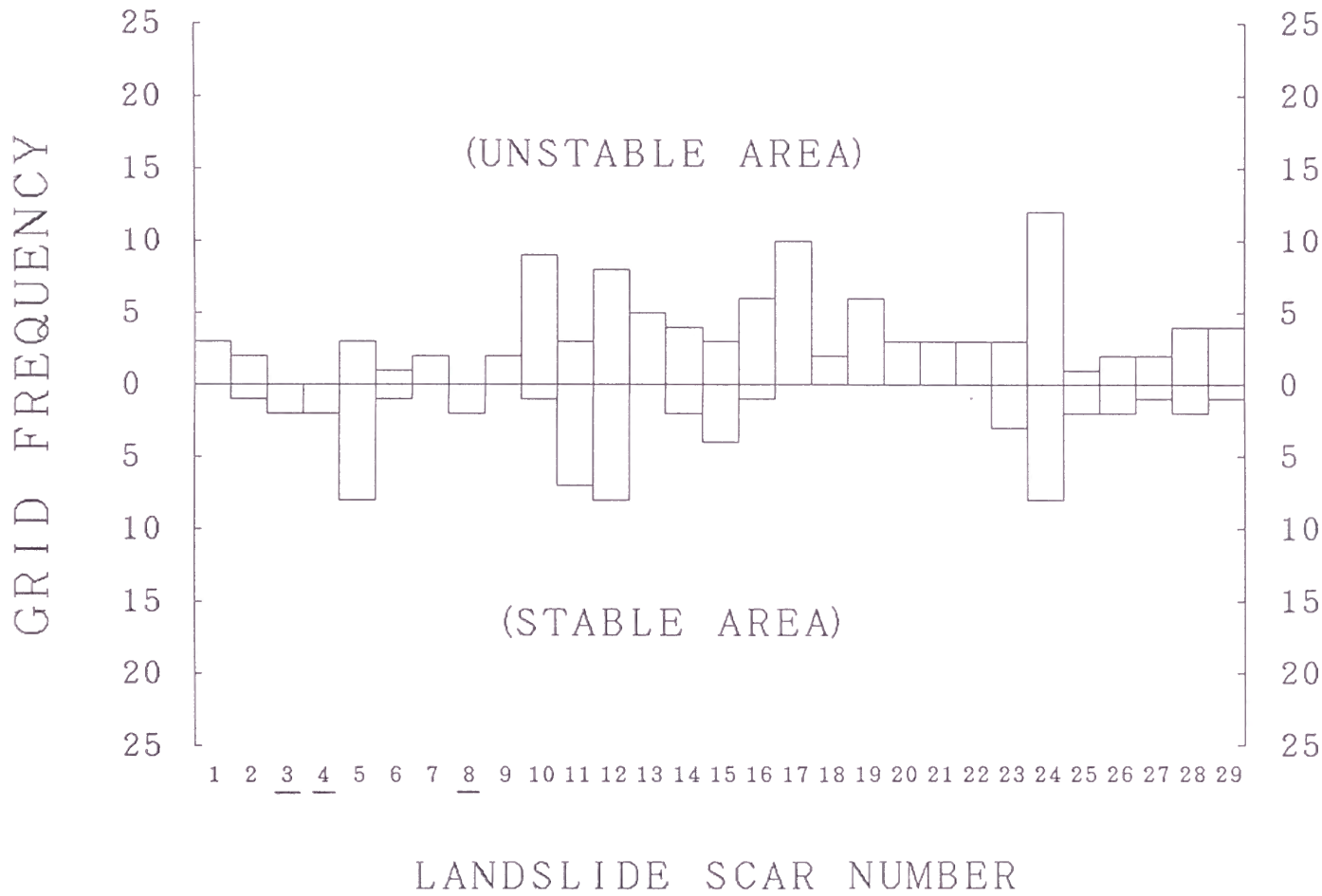

Fig. 10. Comparison of unstable and stable areas in the actual shallow landslide scars (No.1-29 in Fig. 3). The unstable and stable areas are represented by the number of the grid points for which $h_{max} > H_{cr}$ and $h_{max} < H_{cr}$, respectively.

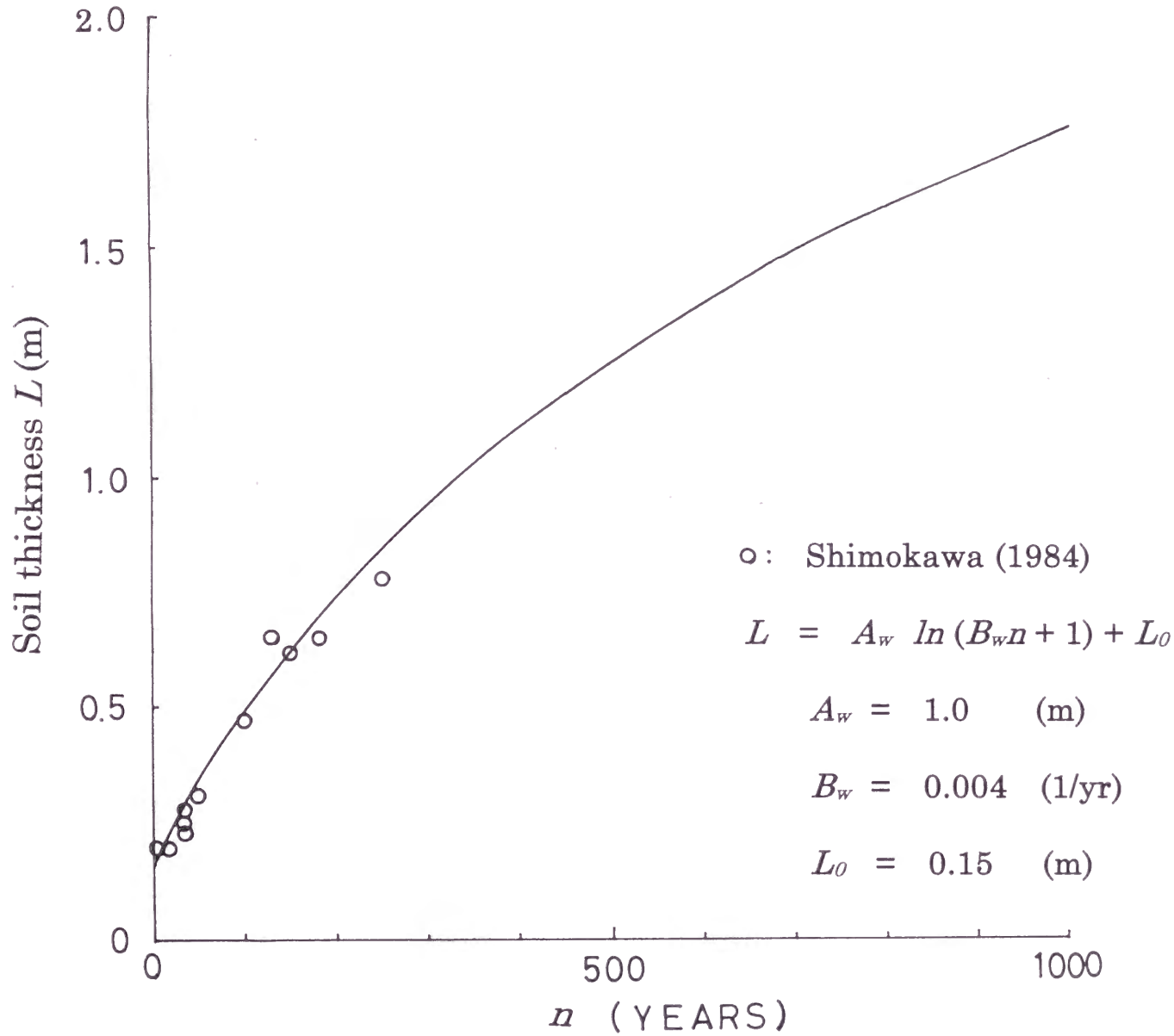

Fig. 11. The growth of soil thickness according to eq. (8) fitted to the data of Shimokawa (1984) and extrapolated up to the period of 1,000 years.

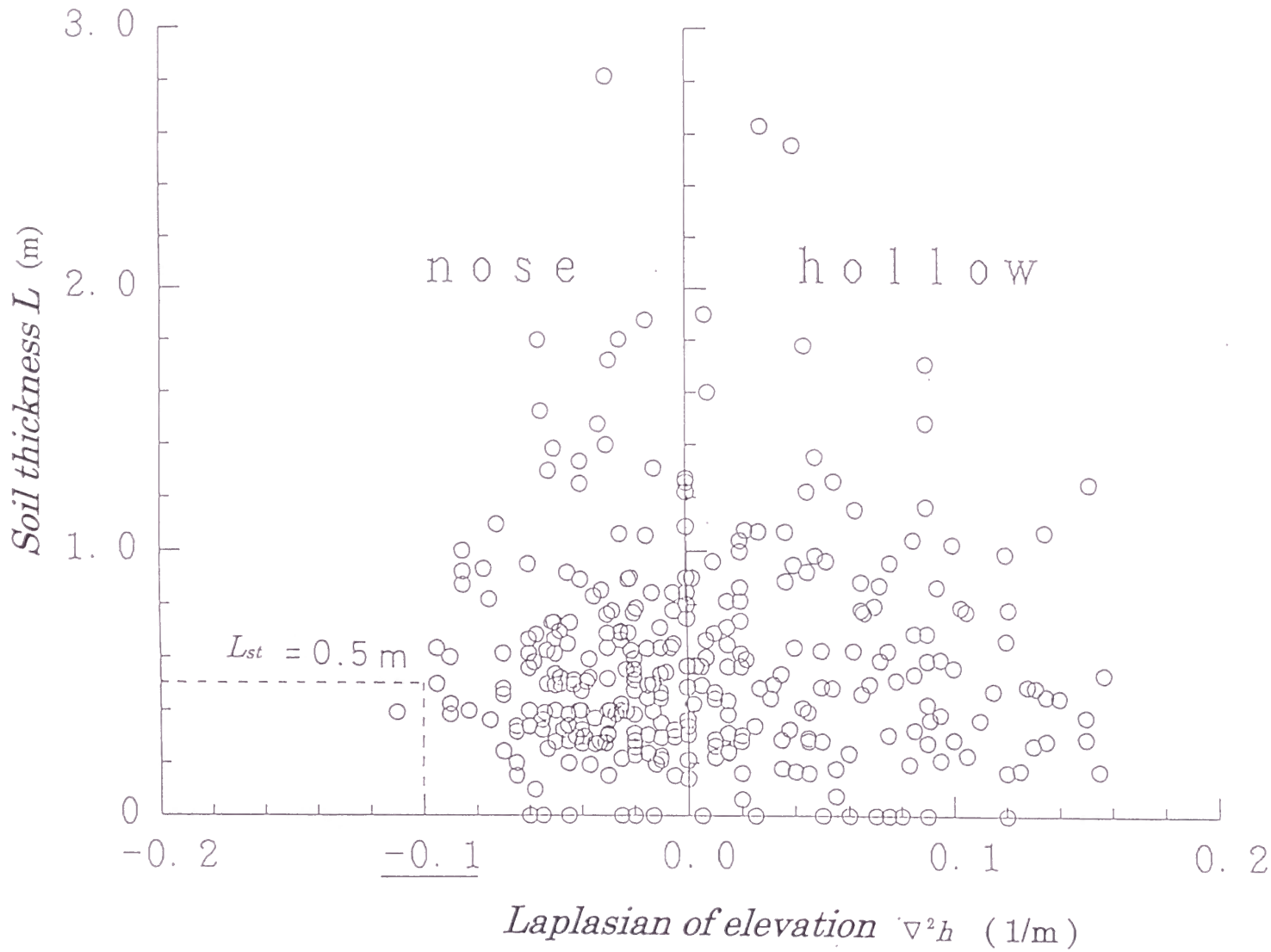

Fig. 12. The relationship between measured soil thickness and laplacian $\nabla^2 h$. Open circles: measured soil thickness (modified from Iida and Tanaka, 1997).

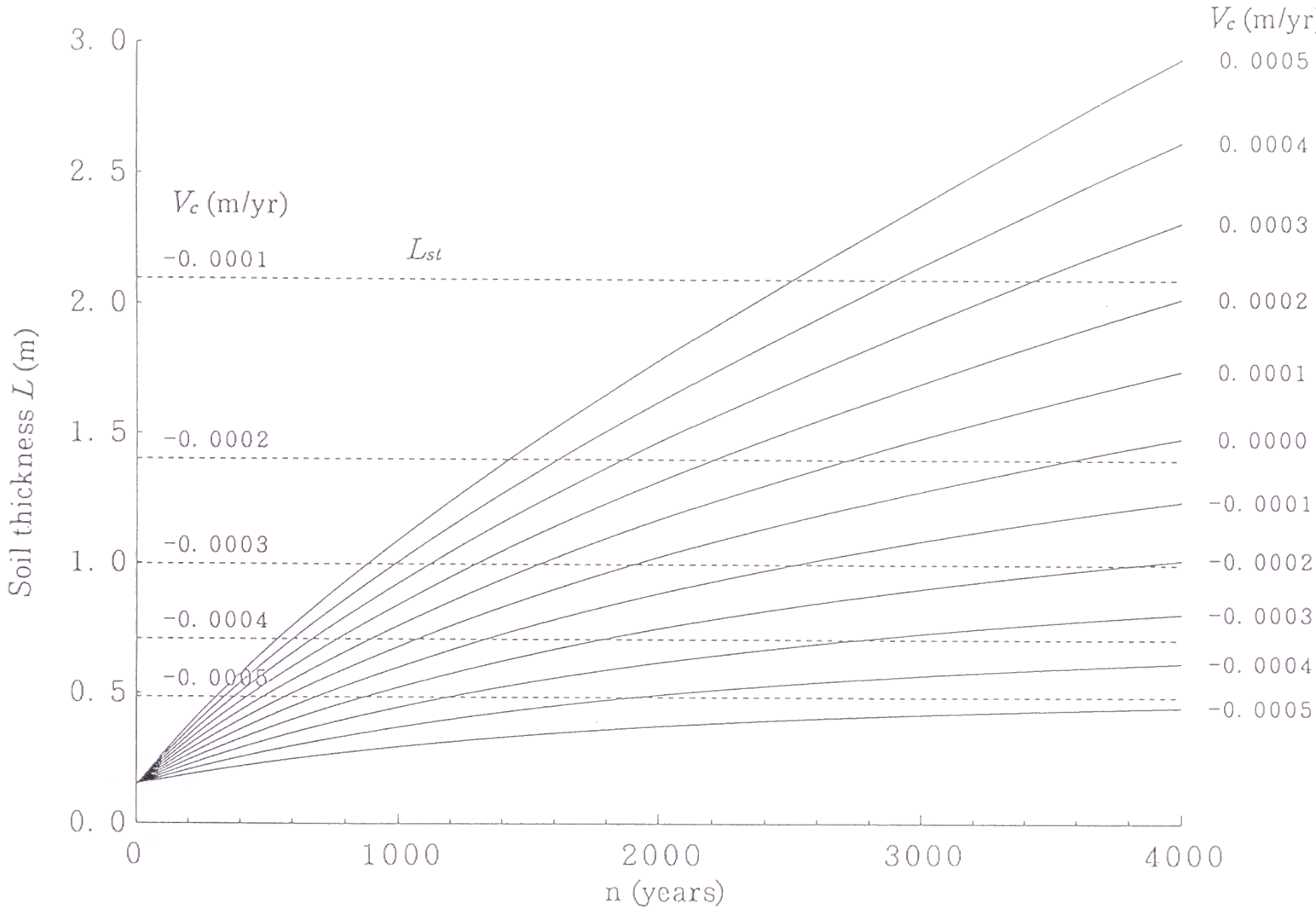

Fig. 13. The time change in the soil depth for the test field for various values of V_c. V_c represents the additional effect by soil creep (eq. (9)' and eq. (10)). Broken lines show the steady state soil thickness L_{st} corresponding to individual values of V_c.

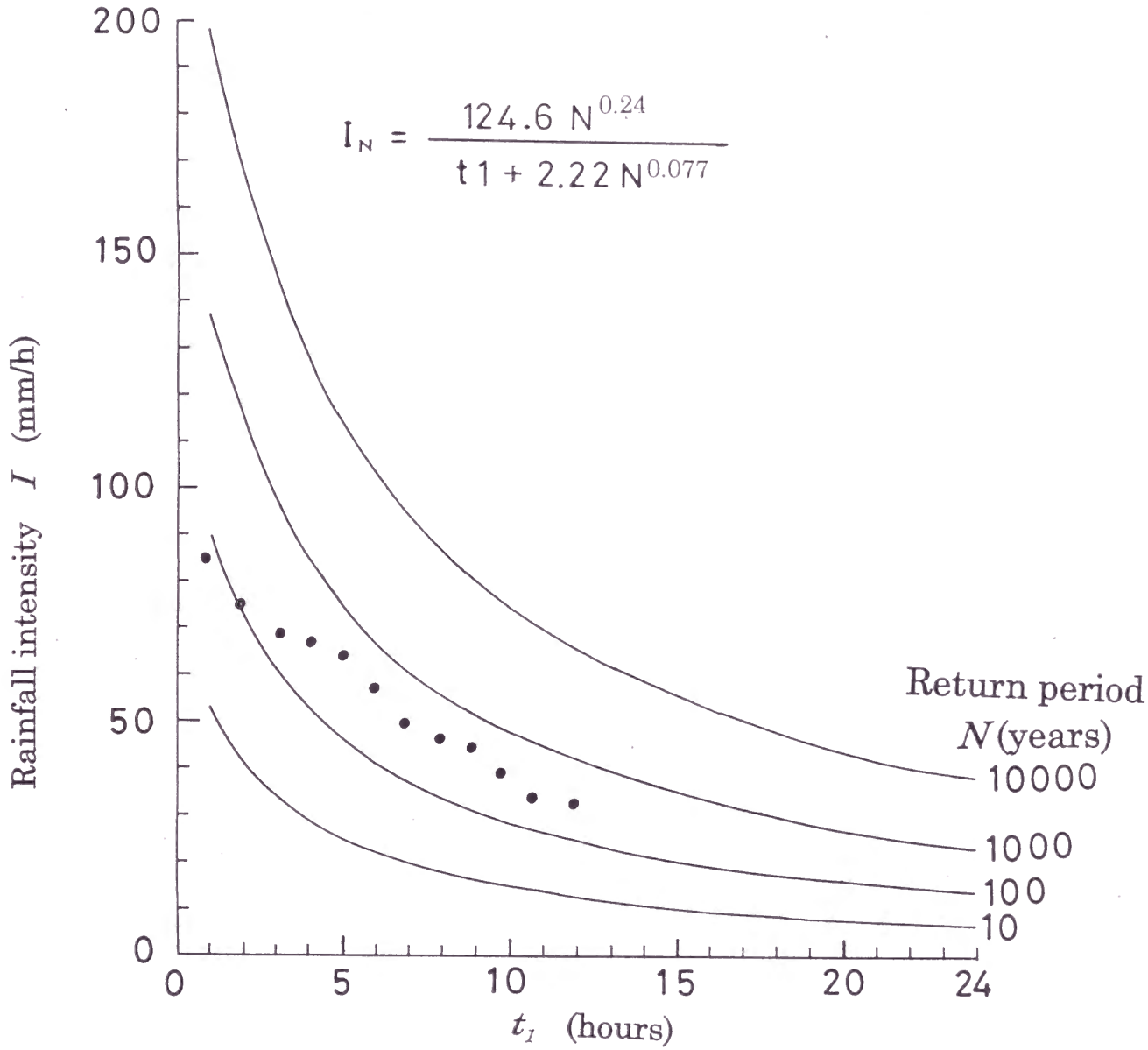

Fig. 14. The stochastic rainfall intensity - duration curves at Hamada Meteorological Observatory near by the test field site for different return periods. Dots: The maximum rainfall intensity versus duration at the 1988 rainstorm (Fig.7).

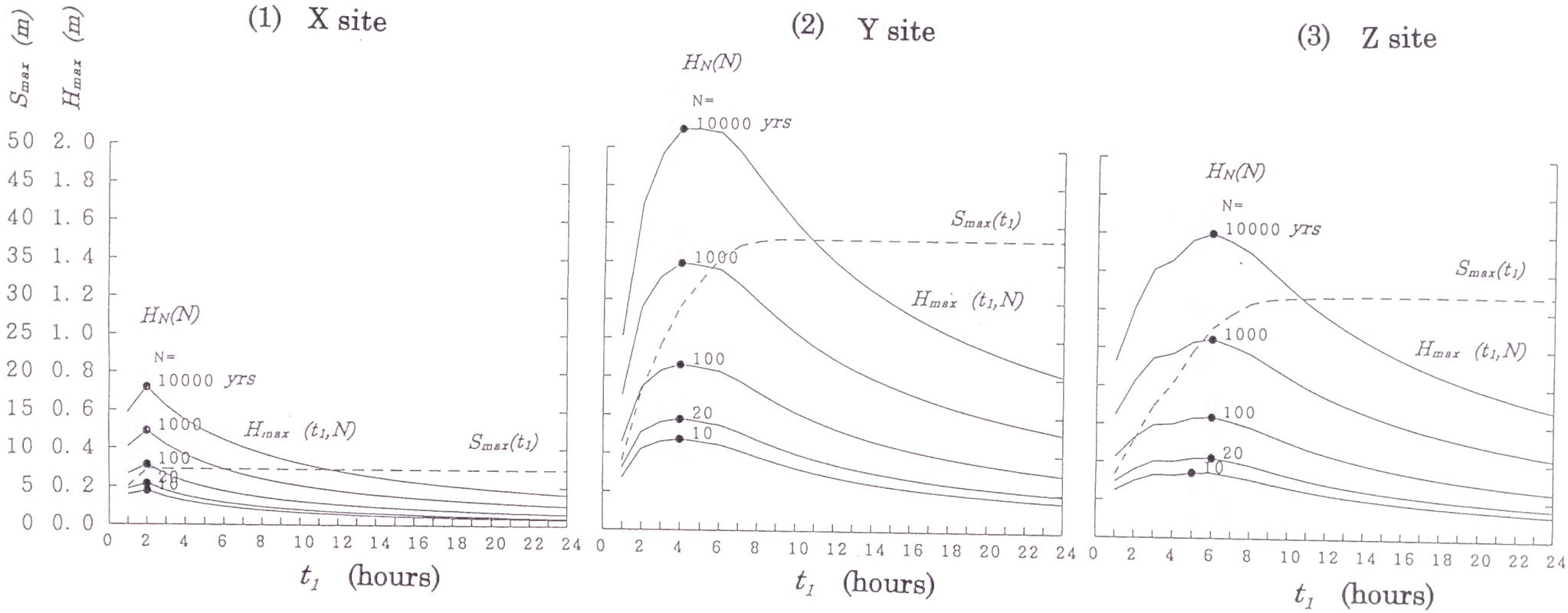

Fig. 15. Examples of $S_{max}(t_1)$ (broken lines) and $H_{max}(t_1,N)$ (solid lines) at the sample sites X,Y and Z in Fig.3. The dots show the peaks of H_{max} $(=H_N)$.

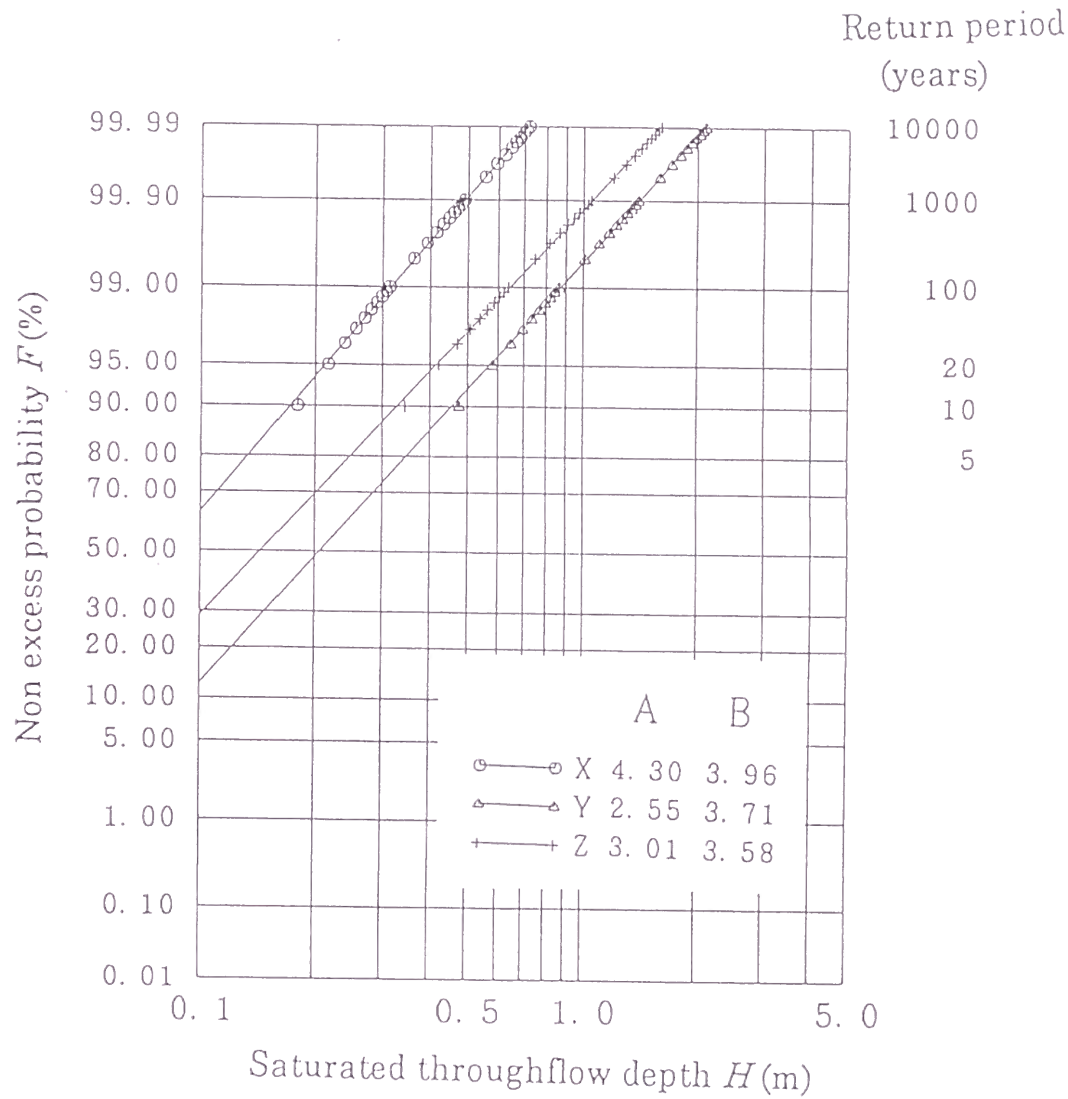

Fig. 16. The probability distribution of throughflow at sample sites X, Y and Z in Fig. 3

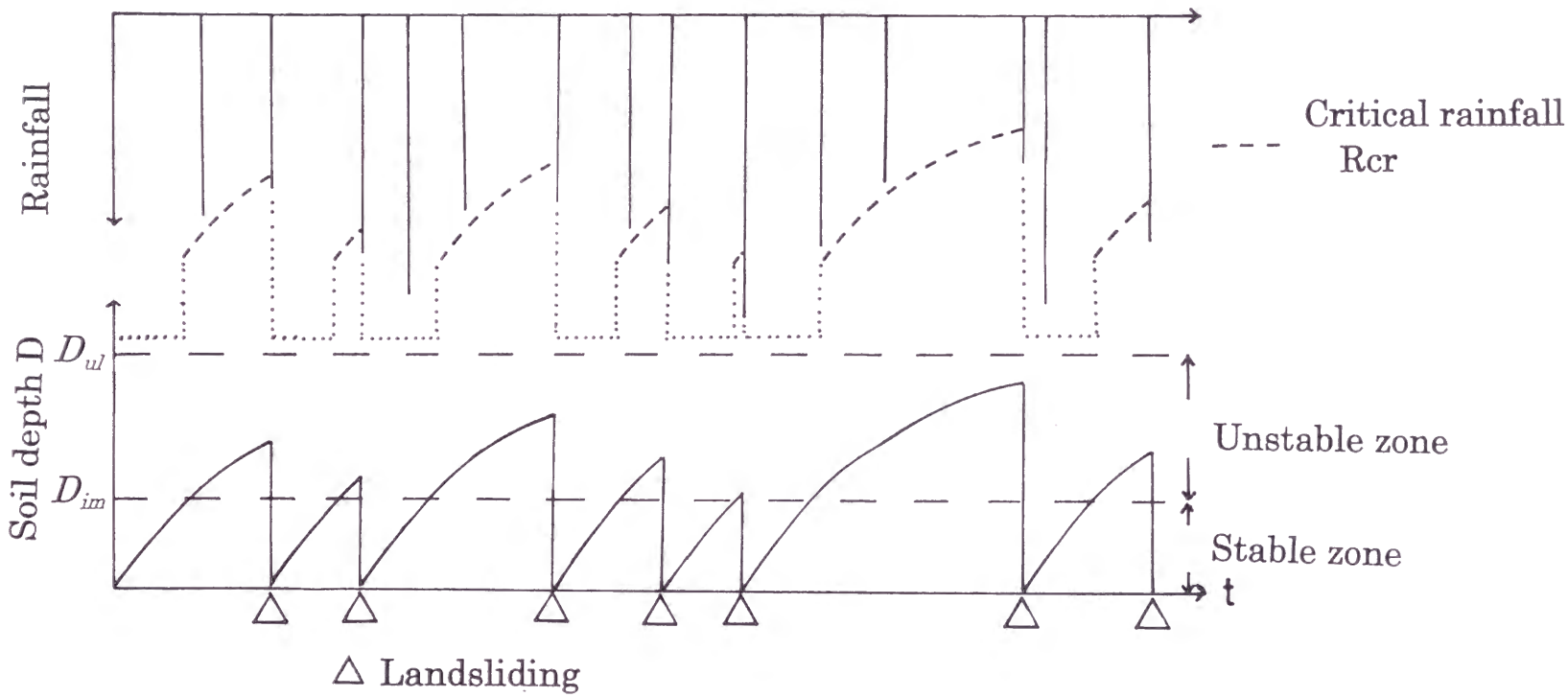

Fig. 17. Schematic illustration of the time change of soil depth D due to landsliding and succeeding recovery. Landslides occur when $D>D_{im}$ and the rainfall attains its critical value R_{cr}. The soil depth D cannot exceed D_{ul} (see the text).

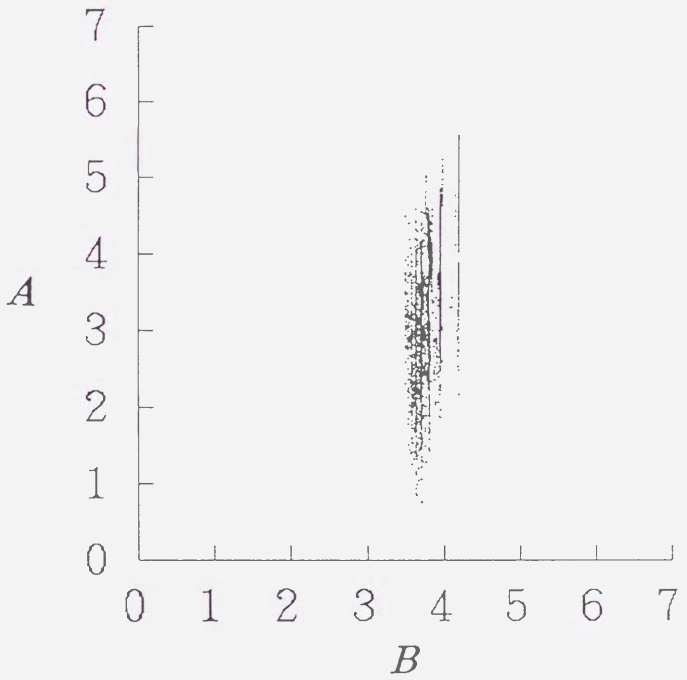

Fig. 18. The correlation between the values of A and B in eq. (15)" obtained in the test field site.

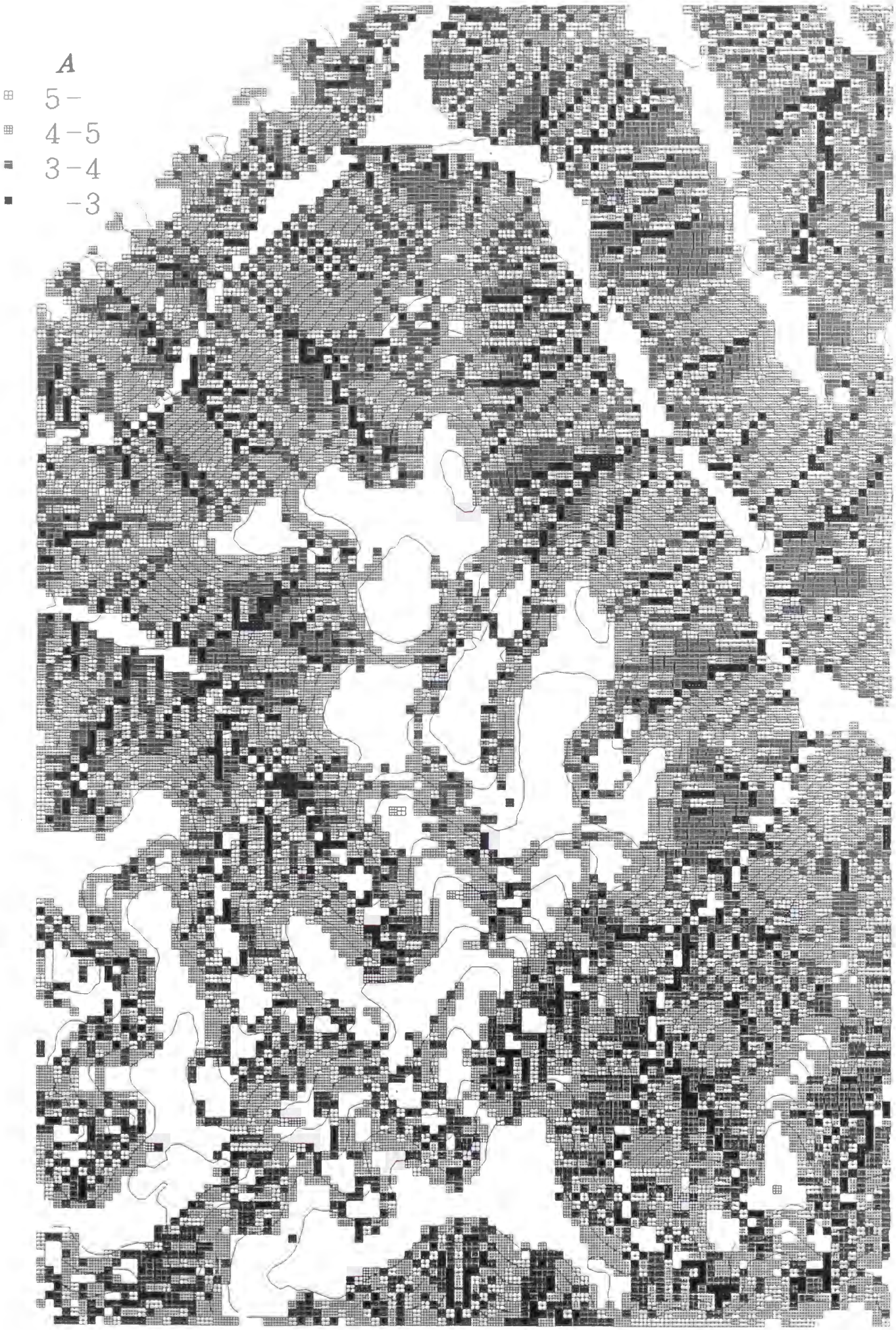

Fig. 19. The distribution of hydro-geomorphological parameter A (eq. (15)").

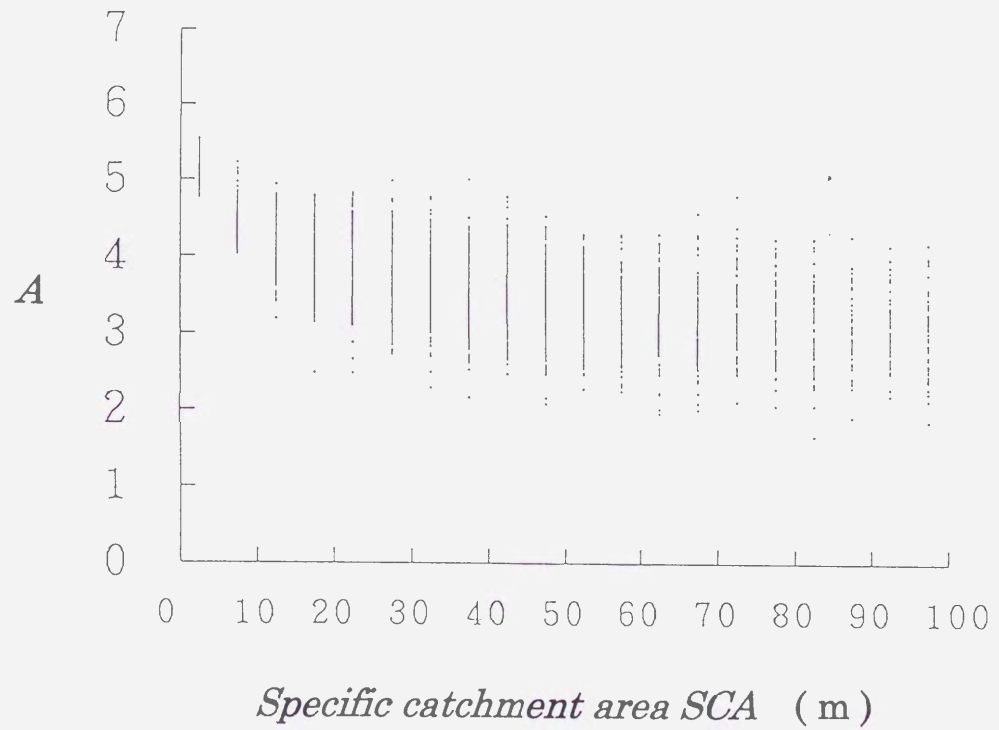

Fig. 20. The correlation between A and Specific Catchment Area (SCA).

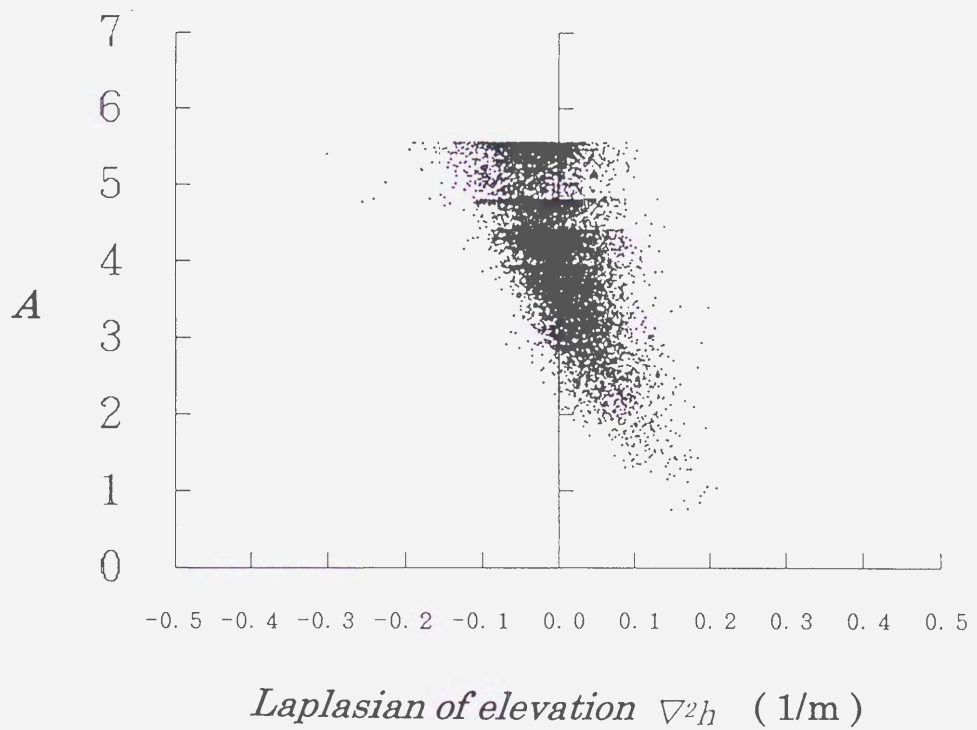

Fig. 21. The correlation between A and laplasian $\nabla^2 h$.

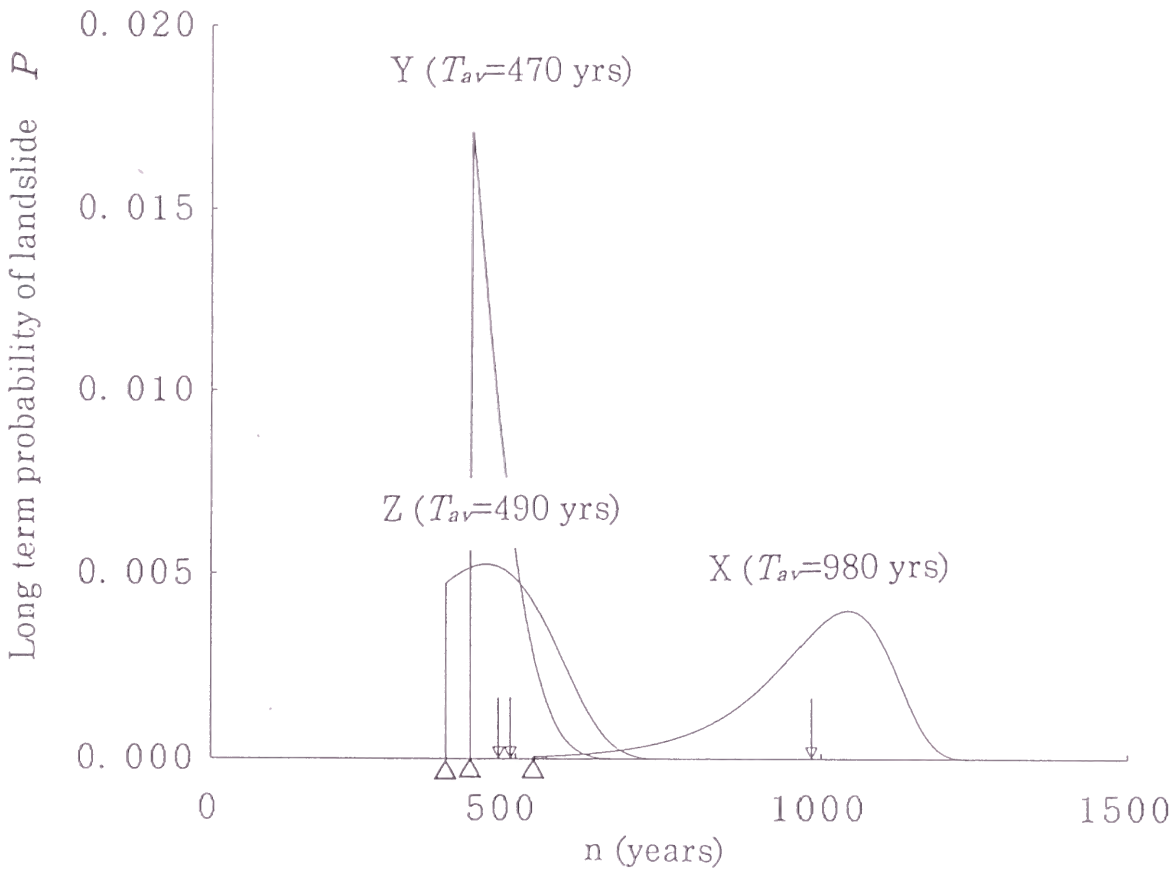

Fig. 22. Examples of the long term probability P as a function of time and the average recurrence interval of landsliding T_{av} (arrows) for the sample sites X,Y and Z in Fig. 3. Triangles show the end of "immunity" periods.

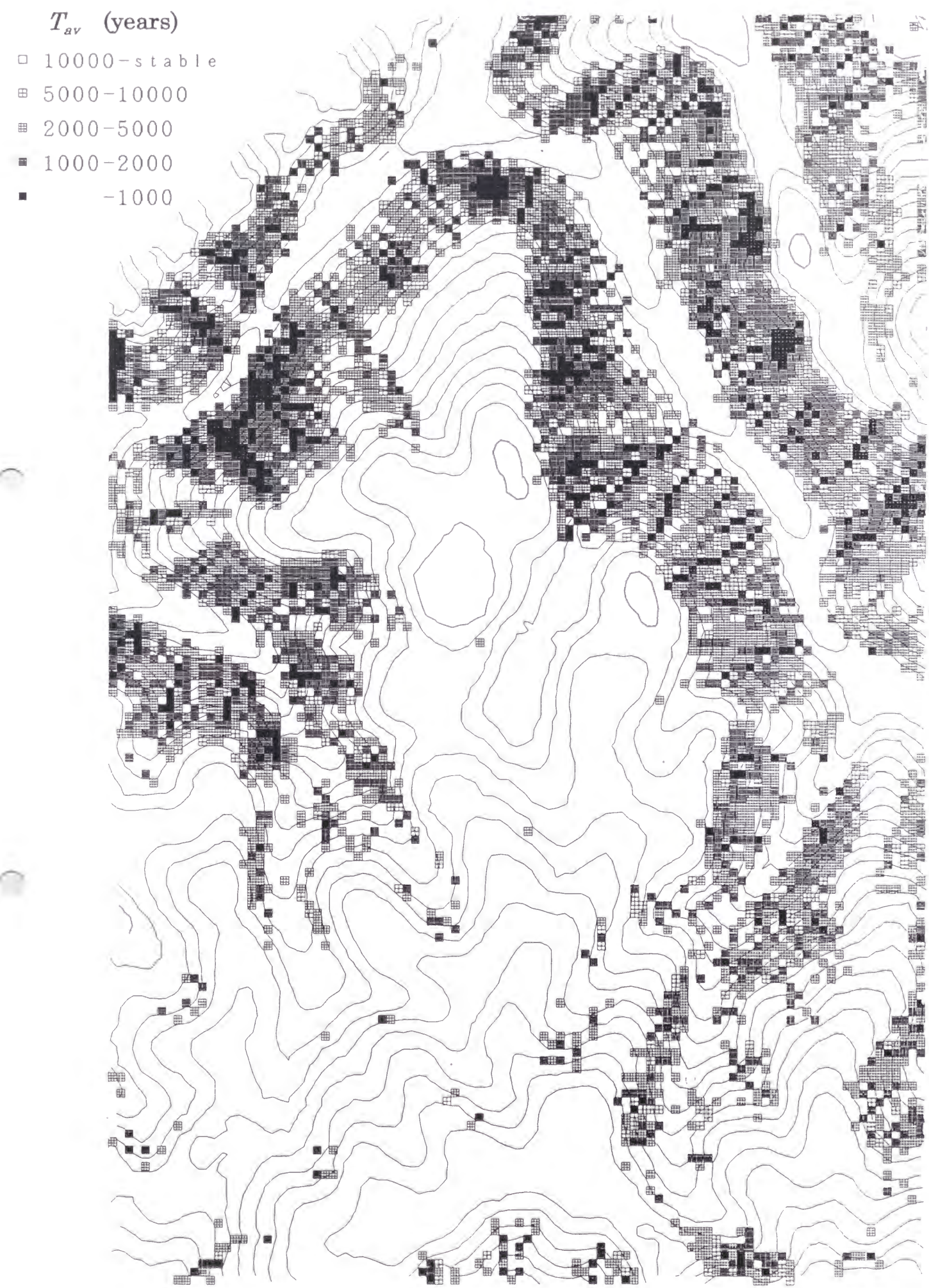

Fig. 23. The distribution of average recurrence interval of shallow landsliding T_{av}.

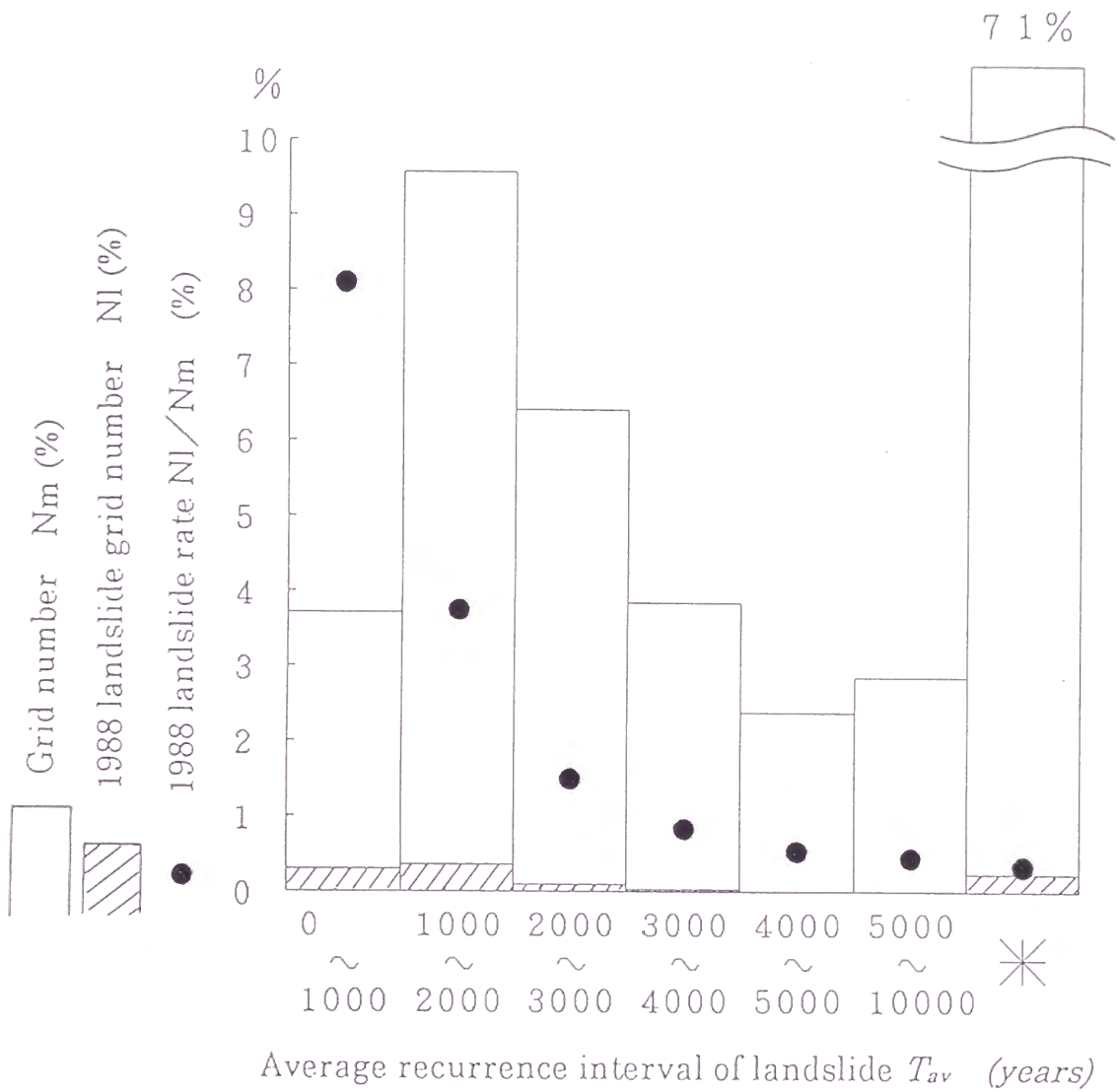

Fig. 24. The relative histogram Nm of the average recurrence interval of shallow landsliding T_{av} evaluated at the grid points in the test field site. Asterisk shows T_{av} >10,000 years or non-landsliding. The shadowed histogram is for the grid points that are involved in the 1988 landslide scars. The dots show the ratio Nl/Nm.

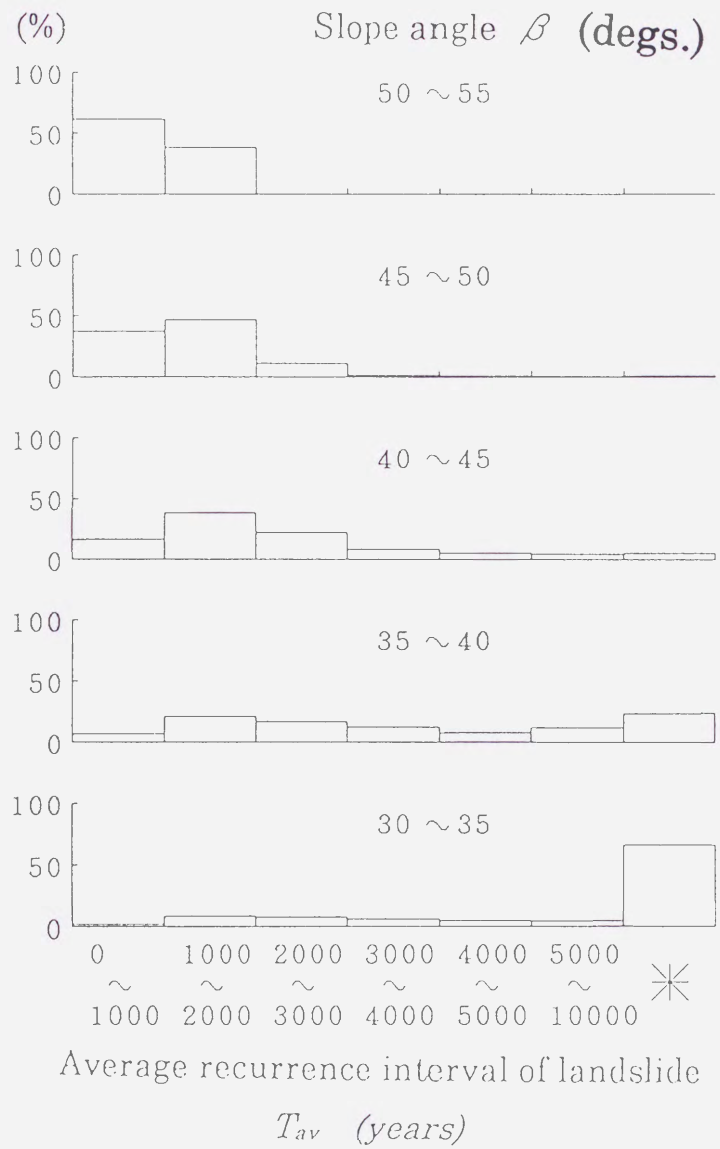

Fig. 25. The relative histogram of the average recurrence interval of shallow landsliding T_{av} for different slope angle rank.

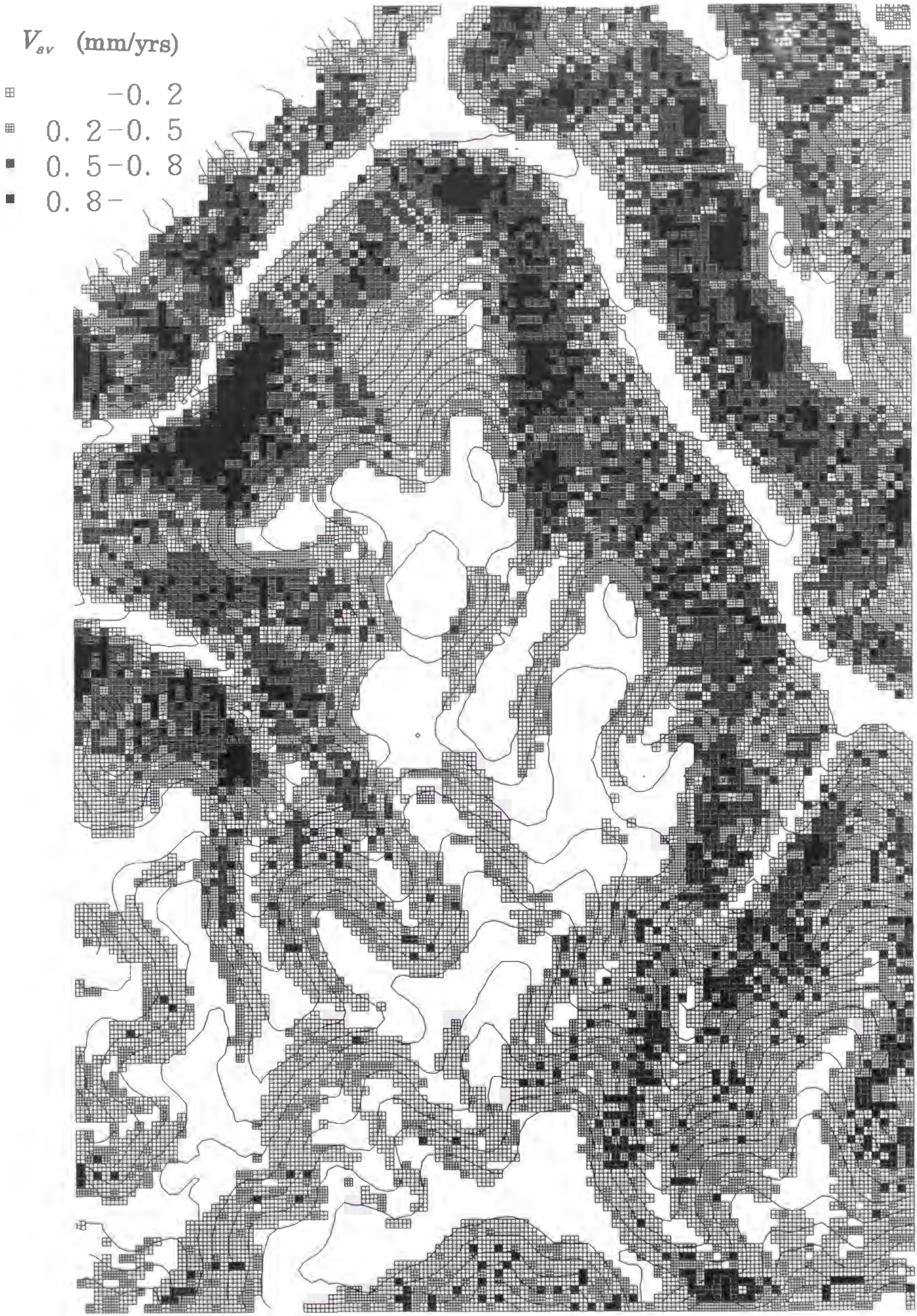

Fig. 26. The distribution of average denudation rate V_{av}.

Table 1. The mechanical, physical and hydrological soil parameters.

c (tf/m^2)	ϕ (degs.)	γ_t (t/m^3)	γ_{sat} (t/m^3)	k (cm/sec)	n_e (%)	α (1/hour)
0.5	30	1.5	1.7	0.1	20	0.4